Observations of cloud liquid water path over oceans: Optical and microwave remote sensing methods

Bing Lin

Columbia University, New York

William B. Rossow

NASA Goddard Institute for Space Studies, New York

Abstract. Published estimates of cloud liquid water path (LWP) from satellite-measured microwave radiation show little agreement, even about the relative magnitudes of LWP in the tropics and midlatitudes. To understand these differences and to obtain a more reliable estimate, optical and microwave LWP retrieval methods are compared using the International Satellite Cloud Climatology Project (ISCCP) and special sensor microwave/imager (SSM/I) data. Errors in microwave LWP retrieval associated with uncertainties in surface, atmosphere, and cloud properties are assessed. Sea surface temperature may not produce great LWP errors, if accurate contemporaneous measurements are used in the retrieval. An uncertainty of estimated near-surface wind speed as high as 2 m/s produces uncertainty in LWP of about 5 mg/cm^2. Cloud liquid water temperature has only a small effect on LWP retrievals (rms errors < 2 mg/cm^2), if errors in the temperature are < 5°C; however, such errors can produce spurious variations of LWP with latitude and season. Errors in atmospheric column water vapor (CWV) are strongly coupled with errors in LWP (for some retrieval methods) causing errors as large as 30 mg/cm^2. Because microwave radiation is much less sensitive to clouds with small LWP (less than 7 mg/cm^2) than visible wavelength radiation, the microwave results are very sensitive to the process used to separate clear and cloudy conditions. Different cloud detection sensitivities in different microwave retrieval methods bias estimated LWP values. Comparing ISCCP and SSM/I LWPs, we find that the two estimated values are consistent in global, zonal, and regional means for warm, nonprecipitating clouds, which have average LWP values of about 5 mg/cm^2 and occur much more frequently than precipitating clouds. Ice water path (IWP) can be roughly estimated from the differences between ISCCP total water path and SSM/I LWP for cold, nonprecipitating clouds. IWP in the winter hemisphere is about 3 times the LWP but only half the LWP in the summer hemisphere. Precipitating clouds contribute significantly to monthly, zonal mean LWP values determined from microwave, especially in the intertropical convergence zone (ITCZ), because they have almost 10 times the liquid water (cloud plus precipitation) of nonprecipitating clouds on average. There are significant differences among microwave LWP estimates associated with the treatment of precipitating clouds.

1. Introduction

The effects of clouds on exchanges of radiative and latent heat energy and freshwater depend on both macrophysical parameters (i.e., horizonal and vertical extent, cloud liquid water path, cloud ice water path, and cloud temperature) and microphysical parameters (i.e., water phase, particle composition, particle size distribution, and shape). At present, it is difficult to observe all of these properties directly or to obtain global information about them. Thus developing more methods to survey additional cloud properties from satellites is important to progress in understanding clouds.

Before the 1980s, comprehensive global observations of cloud optical thickness or water contents did not exist, although the global radiation balance, together with the collection of aircraft observations, provided some estimates of these quantities [*Slingo et al.,*

1982; *Arking,* 1991 and references therein]. Most determinations of liquid water path (LWP) have been made from satellite microwave radiance measurements [*Prabhakara et al.,* 1983; *Njoku and Swanson,* 1983; *Greenwald et al.,* 1992, 1993]. The only systematic microwave survey completed so far is based on Nimbus 7 (SMMR) scanning multichannel microwave radiometer measurements [*Gloersen et al.,* 1984]. Because of the strong and variable effects of land surface properties on the microwave radiances observed from satellites, microwave retrievals of LWP have been limited to open ocean areas. Recently, more effort to estimate LWP has been made using the special sensor microwave/imager (SSM/I) [e.g., *Alishouse et al.,* 1990a; *Petty,* 1990; *Liu and Curry,* 1993; *Greenwald et al.,* 1993]. The algorithms of Alishouse et al. and Petty are derived from observations in limited regions and/or seasons and so must be used with caution for global LWP estimations [see *Liu and Curry,* 1993]. *Liu and Curry* [1993] use observations of clear sky brightness temperatures to represent the microwave radiative contributions of the atmosphere and sea surface and derive a relation between the cloud emissivity and the brightness temperatures for nonprecipitating clouds. For precipitating clouds, LWP is retrieved from their scattering-based microwave radiative transfer model. *Greenwald et al.*

[1993] retrieve column water vapor (CWV) and LWP simultaneously using an emission-based microwave radiative transfer model. We will give more details about this algorithm later. Figure 1 [compare *Greenwald et al.*, 1993] shows the zonal mean LWP retrievals for August using the algorithms of *Prabhakara et al.* [1983], *Njoku and Swanson* [1983], and *Greenwald et al.* [1993]. The estimates derived by the Prabhakara et al. method and by Njoku and Swanson are both based on SMMR measurements, although the Prabhakara et al. method concerns the Nimbus 7 SMMR observations at 6.6 and 10 GHz, while Njoku and Swanson use the Seasat SMMR data with a slightly modified form of the *Wilheit and Chang* [1980] algorithm. The retrievals of Greenwald et al. are obtained from SSM/I data. These published results do not agree even qualitatively.

Many factors influence the LWP values retrieved from microwave radiances, such as column water vapor, cloud liquid water temperature, near-surface wind, and sea surface temperature. If these effects are not accurately accounted for in the analysis, they produce errors in the LWP estimation. Some papers [*Staelin et al.*, 1976; *Curry et al.*, 1990; *Petty*, 1990; *Greenwald et al.*, 1993] have discussed these error sources, but quantitative relationships between the errors and these parameters are not available.

LWP can also be inferred from optical measurements (by which we mean solar wavelengths) of cloud reflectivities and absorptions. The first global analysis of satellite visible radiance measurements to provide average cloud optical thicknesses was reported by *Rossow and Lacis* [1990; see also *Rossow et al.*, 1989]. *Greenwald et al.* [1992, 1993] show good agreement between remotely sensed values of LWP from microwave and visible wavelength (about 0.6 μm) measurements for a few cases of subtropical stratocumulus. *Lojou et al.* [1991] found a strong correlation of the microwave and optically derived LWPs in the tropics, where they used the optical values of LWP as a reference. These studies also reveal that the calibration for both microwave and optical radiances is a key determinant of the accuracy of LWP retrievals. Generally, however, as shown in Figure 1, the average total water path (WP), equal to the sum of LWP and ice water path (IWP), inferred from the average cloud optical thicknesses derived by the International Satellite Cloud Climatology Project (ISCCP) [*Rossow and Schiffer*, 1991] is smaller in magnitude than obtained from microwave methods.

This study is motivated by two questions. (1) Why do the various published microwave-based estimates of LWP differ so much when, at first sight, their methods do not differ so much and (2) why are the average ISCCP-based values of WP lower than the average microwave-based values, when the higher sensitivity of optical measurements to IWP implies the opposite expectation? We use the optical remote sensing method, which we show to be much more sensitive to cloud water than a microwave one, to determine the presence of clouds ("cloud detection") and to evaluate the LWP retrieved from a microwave method. The optical data are visible wavelength radiances from imaging radiometers on meteorological satellites that are analyzed by ISCCP to obtain cloud optical thicknesses. The microwave data come from the SSM/I, which we analyze using a method proposed by *Greenwald et al.* [1992, 1993]. These global (excluding polar regions) data sets are described in section 2 and the analysis methods are described in section 3.

The magnitudes of the effects of uncertainties in the most important geophysical parameters on the microwave LWP retrieval are estimated in section 4. We find that water vapor error has, by far, the most important effect on LWP retrievals. Even more important is the definition of "cloudy" for microwave remote sensing, i.e., the definition of which measurements are included in determining the average LWP. We compare the relative sensitivity of the optical and microwave measurements to the presence of clouds
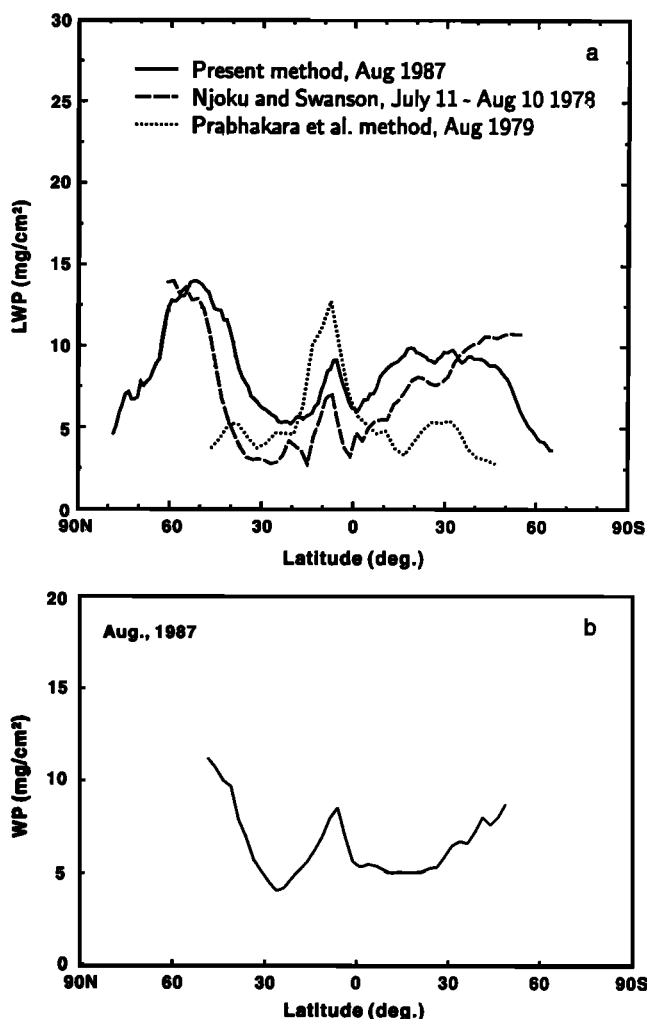
Figure 1. (a) Monthly, zonal mean liquid water path (LWP) values retrieved from three different microwave methods [cf., *Greenwald et al.*, 1993]. The curve "Present method" means the one derived by *Greenwald et al.* [1993]. The observational periods (shown in the figure) for these LWP values are variable but all in July and August. (b) Monthly, zonal mean total cloud water path (LWP + ice water path (IWP)) obtained from the International Satellite Cloud Climatology Project (ISCCP) cloud optical thicknesses for August 1987.

at the end of section 4. Section 5 summarizes the cloud properties inferred from a combination of ISCCP and SSM/I analyses. Finally, in section 6 we list the conclusions from this research.

2. Data Sets

Our study uses two data sets: ISCCP analysis and SSM/I radiances (brightness temperatures). The ISCCP data are used not only to estimate LWP but also to separate clear and cloudy scenes. As we will show, the uncertainties in microwave LWP retrievals make it more difficult for microwave methods to discriminate clear and cloudy scenes. We also take values of useful parameters, such as sea surface temperature (SST) and cloud top temperature, from the ISCCP data set.

The International Satellite Cloud Climatology Project (ISCCP) Data Set

The optical remote sensing data set is from the ISCCP [*Schiffer and Rossow*, 1983]. The ISCCP Global Processing Center ana-

lyzes visible (VIS) and "window" infrared (IR) radiances [*Schiffer and Rossow*, 1983 stage B3 data], together with other data sets, to retrieve cloud properties. The radiances are obtained from the set of polar orbiting and geostationary meteorological satellites operated by several countries. Before producing the standard cloud products [*Rossow and Schiffer*, 1991; *Rossow et al.*, 1991], a "pixel-level" data set (called stage CX) exists that is composed of the stage B3 radiance data, sampled to a resolution of about 30 km and 3 hours, and the complete results of the cloud analysis. The stage CX data set includes the following information for each individual image pixel (which are about 4 – 7 km in size): satellite name, Earth-location, surface type (land/water/coast), snow/ice cover, cloud/no-cloud decision, surface reflectivity and temperature, cloud optical thickness, and top temperature/pressure (if the pixel is cloudy). Clear pixels are defined as those with VIS and IR radiances that do not differ from the inferred VIS and IR radiance values for clear conditions by more than predetermined threshold amounts [*Rossow and Garder*, 1993a]. All other pixels are defined as cloudy. Cloud optical thicknesses are used to estimate LWP. The cloud detection sensitivity in terms of a minimum optical thickness is approximately equal to 0.3 [e.g., *Wielicki and Parker*, 1992].

Microwave Data Set

The SSM/I is carried on the Defense Meteorological Satellite Program (DMSP) polar orbiting, Sun-synchronous satellites, the first of which was launched in June 1987 [*Wentz*, 1988]. SSM/I consists of seven microwave radiometers which measure radiances at frequencies 19.35, 22.235, 37.0, and 85.5 GHz. Both horizontal and vertical polarization measurements are taken at all frequencies except 22.235 GHz (vertical only). The spatial resolution ranges from 70×45 km^2 to 15×13 km^2. Only the lowest three frequencies are used here, because the 85-GHz channels are significantly noisier than the others. The specific advantages of the SSM/I over its predecessors are an improved design and better calibration of the radiometer, higher temporal resolution (twice a day), and larger swath width (1394 km). More detailed specifications of SSM/I can be found in the work of *Hollinger et al.* [1990].

Matching ISCCP and Special Sensor Microwave/Imager (SSM/I) Observations

To match ISCCP and SSM/I observations, we require that the time difference between observations be within ± 1.5 hours (the separation time of ISCCP observations) and that the distance between ISCCP and SSM/I pixels be ≤ 30 km, which is about the resolution of both data sets. This matching process often finds multiple ISCCP pixels for a single SSM/I pixel (or multiple SSM/I pixels for a single ISCCP pixel). For the regional comparison study we retained all matches, even if multiple, to examine the effects of small-scale cloud variability. We found that the major statistical properties of the comparison did not depend on whether the matches were restricted to a single matched pair. For the global analysis and intercomparison we restrict the matches to the ISCCP and SSM/I pixel pair with the minimum separation distance in cases of multiple matches.

3. Liquid Later Path (LWP) Estimation Schemes

Liquid water path, LWP, is the total column liquid water content per unit area. We distinguish between the atmospheric liquid water path, atmosphere-LWP, which is averaged over all areas, including cloud-free locations, and the cloud liquid water path, cloud-LWP, averaged only over cloudy areas. When we mean either or both quantities, we will use LWP. Likewise, we refer to the total atmos-

pheric ice water path, atmosphere-IWP, the cloud ice water path, cloud-IWP, or the ice water path, IWP. The total water path, which may contain both IWP and LWP, is called total-WP. Total column water vapor is called CWV.

Optical Method

In plane-parallel, single-layered clouds the optical thickness for shortwave radiation is directly related to LWP [*Stephens et al.*, 1978; *Stephens*, 1984]. From radiative transfer theory [*Hansen and Travis*, 1974] the optical thickness τ can be expressed as

$$\tau = \int_{z_b}^{z_t} \int_0^{\infty} Q_{ext}(x) n(r) \pi r^2 \, dr \, dz \tag{1}$$

where $x = 2\pi r/\lambda$ is scattering size parameter, λ is the wavelength, r is cloud particle size, z_b and z_t are the heights of the bottom and the top of the clouds, n(r) is droplet size distribution, and $Q_{ext}(x)$ is the extinction coefficient, determined from Mie theory (approximately 2 for typical cloud particle sizes; see, for example, Stephens 1984). Assuming that Q_{ext} is approximately constant over the range of cloud particle radii,

$$\tau \approx Q_{ext} \int_{z_b}^{z_t} \int_0^{\infty} n(r) \pi r^2 \, dr \, dz \tag{2}$$

The mean effective radius of the particle, r_e, is [*Hansen and Travis*, 1974]:

$$r_e = \frac{\int_0^{\infty} \pi r^3 n(r) \, dr}{\int_0^{\infty} \pi r^2 n(r) \, dr} \tag{3}$$

Combining equations (2) and (3) gives

$$\tau \approx \frac{Q_{ext} \int_{z_b}^{z_t} \int_0^{\infty} \pi n(r) r^3 \, dr \, dz}{r_e}$$

$$= \frac{3 Q_{ext} \int_{z_b}^{z_t} dz \int_0^{\infty} \frac{4}{3} \pi r^3 n(r) \, dr}{4 r_e}$$

$$= \frac{3 Q_{ext}}{4 r_e \rho_w} \int_{z_b}^{z_t} \omega \, dz$$

where ω is equal to liquid water content and ρ_w water density. Since the integral of water content over height is cloud-LWP,

$$\tau \approx \frac{3 Q_{ext} \text{LWP}}{4 r_e \rho_w} \tag{4}$$

Finally,

$$\text{cloud-LWP} \approx \frac{4\tau r_e \rho_w}{3Q_{ext}} . \tag{5a}$$

In the ISCCP data the optical thickness τ is retrieved from the measured VIS reflectance for each cloudy image pixel. The ISCCP radiative transfer model [*Rossow et al.*, 1989] represents clouds as single homogeneous layers with an assumed gamma size distribution of spherical water particles. The full effects of multiple scattering and absorption are accounted for in the model. Equation (3) shows that the effective radius r_e is an integrated property of the whole cloud particle size distribution; hence it does not usually change a lot. In the ISCCP model, r_e is assumed to be 10 µm, which is consistent with mean values from recent observations of water clouds to within $1 - 2$ µm [*Han*, 1992; *Han et al.*, 1994; *Luo et al.*, 1994]. With these assumptions, equation (5a) becomes

$$\text{cloud-LWP} \approx 0.6293\tau \ (\text{mg/cm}^2) . \tag{5b}$$

Ice particles influence cloud visible reflectivity only a little less effectively than water droplets. Thus ice clouds are also detected in the ISCCP analysis and contribute to the total cloud water path. In the ISCCP retrieval of cloud optical thicknesses, all clouds are treated as composed of 10-µm liquid water spheres, even though cloud ice particles are usually larger than cloud water droplets and nonspherical in shape [*Heymsfield and Donner*, 1990; *Heymsfield*, 1977; *Hobbs and Rangno*, 1985]. Recent studies show that the ISCCP values of τ for optically thin, ice clouds are overestimated by about $25 - 50\%$ [*Wielicki et al.*, 1990; *Baum et al.*, 1992; *Minnis et al.*, 1993]; for optically thick clouds, with ice contributing significantly to the total optical thickness, the errors are expected to be smaller. The underestimate of r_e is generally greater than the overestimate of τ, so the ISCCP estimated IWP is probably lower than real IWP by factors $2 - 3$ at least.

When rain is present below a cloud, it is formed of very large droplets (> 100 µm) which scatter shortwave radiation much less efficiently than smaller droplets. Since rain is usually produced in clouds with very large cloud-LWP (more than 30 mg/cm²), the column optical thickness is already very large. Even though VIS reflectivity measurements remain sensitive to changes in cloud-LWP up to about 80 mg/cm², optical remote sensing methods significantly underestimate the total LWP for precipitating clouds [e.g., *Wiscombe et al.*, 1984; *Wiscombe and Welch*, 1986].

Microwave Retrieval Method

Wilheit et al. [1977] constructed a theoretical microwave radiative transfer model that includes only cloud emission and absorption. Many other emission-based, semiempirical, or simplified radiative models have been proposed [e.g., *Wilheit and Chang*, 1980; *Prabhakara et al.*, 1982, 1983; *Njoku and Swanson*, 1983; *Takeda and Liu*, 1987; *Alishouse et al.*, 1990a, b; *Petty*, 1990; *Tjemkes et al.*, 1991]. More rigorous radiative transfer models have also been developed, though the final analysis schemes still involve some empirical elements to compensate for physical constants that are not well known [e.g., *Greenwald et al.*, 1992, 1993]. Techniques including the scattering produced by precipitation-sized particles have been used to estimate heavy rain rates [e.g., *Spencer*, 1986; *Smith et al.*, 1992; *Liu and Curry*, 1992].

The SSM/I LWP retrieval scheme used here is an emission-absorption model similar to those just mentioned and was developed by Greenwald et al. and reported at a conference [*Greenwald et al.*, 1992]. This scheme retrieves LWP and column water vapor (CWV) simultaneously, using the following linear equations:

$$k^{V19} \text{CWV} + k^{L19} \text{LWP} = -0.5\mu \ \ln \ \left[\frac{T_{19h} - T_{19v}}{T_s R_{19v}(1 - R_{19hv})t_{o19}^2}\right] \tag{6}$$

$$(k^{V37} - k^{V19}) \text{CWV} + (k^{L37} - k^{L19}) \text{LWP} \tag{7}$$

$$= -0.5\mu \ \ln \ \left[\frac{(T_{37v} - T_{37h})}{(T_{19v} - T_{19h})} \frac{(\varepsilon_{19v} - \varepsilon_{19h})}{(\varepsilon_{37v} - \varepsilon_{37h})} \frac{t_{o19}^2}{t_{o37}^2}\right]$$

where t_{oi}, ε_{ij}, and T_{ij} are the transmittance of oxygen, the sea surface emissivity and the brightness temperature of j polarization at i frequency, respectively. R_{19v} is the sea surface reflectance and R_{19hv} is equal to $(T_{19h} - T_s)/(T_{19v} - T_s)$, where T_s is the sea surface temperature; k^{Li} and k^{Vi} are liquid water and water vapor absorption coefficients at i frequency; μ is equal to $\cos\Theta$, where Θ is the angle between vertical and propagation. In our calculation the values of t_{oi} and k^{Vi} are from *Greenwald et al.* [1992] (i.e., $t_{o19} = 0.982$, $t_{o37} = 0.935$, $k^{V19} = 2.33 \times 10^{-3}$ kg⁻¹m², $k^{V37} = 2.46 \times 10^{-3}$ kg⁻¹m²), and the liquid water absorption coefficients, which are sensitive to cloud liquid water temperature, are calculated from the *Petty* [1990] formulae. In the Greenwald et al. scheme, the cloud temperature is given by $T_s - 8$ K; we explore the effects of using the ISCCP cloud top temperature information instead.

Greenwald et al. changed this scheme in several ways before submitting their formal paper [*Greenwald et al.*, 1993]. Two parameters changed values slightly: the cloud temperature offset from T_s was changed to 6 K and the value of $k^{V37} = 2.11 \times 10^{-3}$ kg⁻¹m². In addition, instead of using equation (7), which represents the difference between the absorptions at 19 and 37 GHz, they use a "direct" equation like (6) for 37 GHz. Sensitivity tests (see next section) show that the scheme used here is less sensitive to uncertainties in sea surface temperature.

These two sets of equations are theoretically similar, but as we discuss, their sensitivity to errors in other parameters is somewhat different when used for LWP and CWV retrievals. This arises because equations (6) and (7), or two equations like (6), couple the accuracy of the CWV retrieval directly to the accuracy of the LWP retrieval and vice versa. Equation (6) is a slightly different form of the expression used by *Tjemkes et al.* [1991] to retrieve CWV under clear conditions (LWP = 0), although no method to identify clear conditions from microwave measurements was proposed. Equations (6) and (7) can be derived from emission models, if there are no precipitating clouds [*Liou*, 1980; *Tjemkes et al.*, 1991; *Greenwald et al.*, 1992, 1993]. Equation (6) is preferable for retrieval of CWV because the first term on the left is usually larger than the second. Similarly, equation (7) can be used to retrieve LWP by specifying climatological values of CWV, because the second term is larger than the first. Thus LWP and CWV can be retrieved simultaneously or separately. However, because CWV is much larger than LWP, if both are expressed in the same units, the differences in magnitude of the terms in equations (6) and (7) are not so large that the other terms on the left can be neglected. We evaluate the sensitivities of several approaches in the next section.

When it is raining, especially in severe thunderstorms, scattering of microwave radiation by the large precipitation particles becomes significant and equations (6) and (7) are no longer accurate [*Liou*, 1980; *Spencer*, 1986; *Wilheit et al.*, 1991; *Adler et al.*, 1991; *Smith et al.*, 1992]. Microwave radiation is insensitive to ice particles if their radii are less than about 150 µm [*Wilheit et al.*, 1977; *Mugnai and Smith*, 1988; *Smith and Mugnai*, 1988; *Wilheit et al.*, 1991; *Adler et al.*, 1991]. The exact effects of large ice and liquid water

particles on the radiation are not yet clear. For the three lower frequencies of SSM/I, such particles produce only weak scattering effects [*Wilheit et al.*, 1991]. The method used to determine the presence of precipitation is $T_{37v} - T_{37h} < 37$ K corresponding to the Goodberlet et al. rain flag is equal to 2 or 3 (compare next paragraph and Table 1).

The sea surface emissivity used in equations (6) and (7) is derived from the *Pandey and Kakar* [1982] expression and the *Klein and Swift* [1977] model. For sea surface temperature we use values from ISCCP, which differ little from other data sets [*Rossow and Garder*, 1993b]. Near-surface wind speed (W) is estimated from the measurements at 19, 22, and 37 GHz for both clear and cloudy conditions using an empirical formula [*Goodberlet et al.*, 1990]:

$$W = 147.90 + 1.0969T_{19v} - 0.4555T_{22v} \qquad (8)$$
$$- 1.7600T_{37v} + 0.7860T_{37h}$$

This formula not only estimates wind speed but also indicates the accuracy of the estimated speed using a rain flag (Table 1), which mostly depends on the local weather conditions. Combining the wind speed and the rain flag, we can evaluate the atmospheric conditions, i.e., calmness, windiness, and presence of rain, which produce significant changes in the microwave radiation.

4. Assessment of Microwave Retrieval Errors

We check the influence on LWP retrievals of uncertainties in sea surface temperature (T_s), near-surface wind speed (W), cloud liquid water temperature (Tc), and column water vapor (CWV). *Staelin et al.* [1976], *Curry et al.* [1990], and *Greenwald et al.* [1993] have also examined these effects but do not give quantitative assessments. We suggest some strategies for minimizing LWP errors caused by these factors in section 6.

We compare values of LWP obtained from the optical and microwave methods for the case where they are expected to agree very well, namely, for warm, nonprecipitating, stratiform clouds which are nearly plane-parallel, single-layered liquid water clouds with narrow droplet size distributions. In particular, we examine results for October 1987 near the surface site providing the validation used by *Greenwald et al.* [1992, 1993]: 31°N – 36°N, 238°E – 243°E. We also compare the two methods for the whole month of November 1987. Since the cloud-LWP values of the optical and microwave method generally agree for this cloud type (see below), we use the comparison results to illustrate the sensitivity studies by showing the effects of parameter uncertainties on the differences between the SSM/I and the ISCCP values of cloud-LWP.

Table 1. Rain Flag in Sea Surface Wind Speed Estimation

| Rain Flag	Criteria	Errors, m/s
0	$T_{37v} - T_{37h} > 50$ $T_{19h} < 165$	< 2 m/s
1	$T_{37v} - T_{37h} < 50$ $T_{19h} > 165$	2 – 5 m/s
2	$T_{37v} - T_{37h} < 37$	5 – 10 m/s
3	$T_{37v} - T_{37h} < 30$	> 10 m/s

Rain flag in near sea surface wind speed estimation [*Goodberlet et al.*, 1990]. In this paper, rain flags 0 and 1 are assumed to be nonprecipitating cases, while flags 2 and 3, precipitating cases.

The baseline microwave retrieval scheme for the sensitivity tests uses the ISCCP results to separate matched SSM/I pixels into cloudy and clear groups. Equation (6) with LWP = 0 is used to retrieve CWV from the clear SSM/I pixels. Then equation (7) is used to obtain estimates of LWP for the cloudy SSM/I pixels with CWV values assumed equal to those for nearby clear conditions, defined by the mean CWV values in 1° × 1° or 2.5° × 2.5° grid boxes at the nearest time. Cloud water temperatures are specified by the ISCCP cloud top temperatures. Sea surface temperature values are specified from ISCCP and the near-surface wind speed values are obtained for each pixel using equation (8). Global (excluding the polar regions) LWP values are discussed in the next section.

Effects of Uncertainties in T_s and Near-Surface Wind Speed

The ocean surface is a major source of the radiation observed by the satellite microwave radiometer; the amount depends on the temperature, T_s, and emissivity of the ocean surface; the latter quantity depends on the near-surface wind speed, W. Since SSM/I lacks the lower-frequency channel (< 10 GHz) that was available on SMMR, direct retrievals of T_s are difficult, especially under cloudy conditions [*Wilheit and Chang*, 1980; *Njoku and Swanson*, 1983; *Prabhakara et al.*, 1983]; thus for SSM/I analyses, values of T_s must be specified from other data sets or from climatology. Retrievals of W are significantly affected by clouds and precipitation [*Wentz et al.*, 1986]; but *Goodberlet et al.*'s [1990] method appears to work well except when significant precipitation is present.

Figure 2 shows the effects of varying only the T_s values by ± 5 K on the comparison of SSM/I and ISCCP values of LWP. In equation (7), T_s is only an implicit parameter, affecting the brightness temperature difference ratio, which has little direct effect on the LWP retrieval. The uncertainties in LWP associated with uncertainties in T_s are therefore negligible (<1 mg/cm²), even for ± 5 K T_s errors
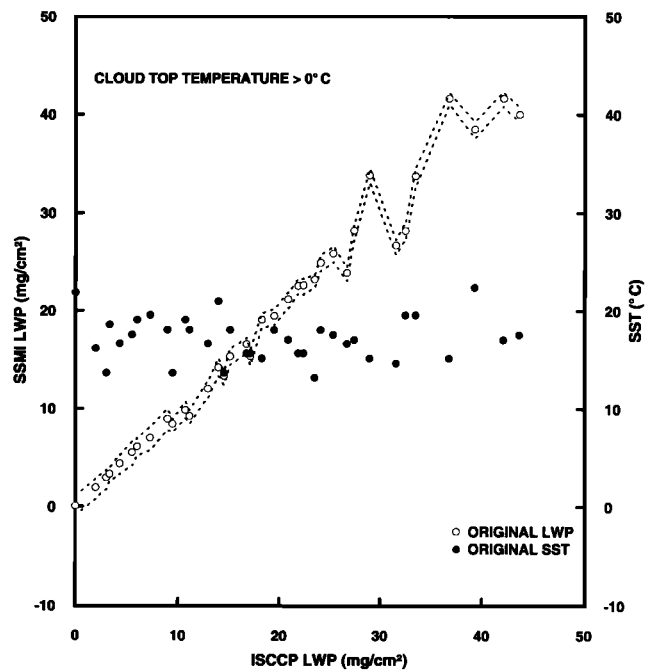
Figure 2. Effect of varying sea surface temperature on retrieved LWP (in unit mg/cm²), using equation (7). The open circles are the original estimated LWPs and the solid circles are the original T_s values. Abscissa is LWP derived from ISCCP and vertical axis is the LWP from the special sensor microwave/imager (SSM/I). The LWPs for changed T_s (±5°C) are represented by dashed curves.

(Figure 2). However, sea surface temperature appears in equation (6) and has a direct effect on the retrieval of CWV, which was held fixed for the experiments shown in Figure 2. So in practice, the more important effect of T_s uncertainties on LWP values is felt through its effect on CWV retrievals and the coupling between CWV and LWP, which we consider later. Similar results were also discussed by *Greenwald et al.* [1993]. Because the ISCCP values of T_s are generally accurate to within 2 – 3 K [*Rossow and Garder,* 1993b], the associated direct uncertainties in LWP are much less than produced by other parameters.

In the LWP retrieval scheme the terms R_{19v} and $(\epsilon_{19v} - \epsilon_{19h})/(\epsilon_{37v} - \epsilon_{37h})$ (denoted hereafter by DEMS) depend on W. Figure 3 shows that their variation over wind speeds of 0 – 40 m/s is generally < 10%. Note that a minimum in DEMS occurs at a wind speed around 8 m/s, so that the sign of the error in LWP associated with an error in wind speed around this value is always positive, regardless of whether the wind speed is underestimated or overestimated. Since climatological near-surface wind speeds are in the range of 3 – 10 m/s; this behavior means that random wind speed errors can produce biased LWP values.

To understand the sensitivity of LWP to uncertainties of near-surface wind speed, we consider the derivatives of equations (6) and (7), i.e.,

$$\delta LWP_1 = 0.5\mu\delta R_{19v}/(k^{L19} \cdot R_{19v})$$

$$\delta LWP_2 = -0.5\mu\delta DEMS/[(k^{L37} - k^{L19}) \, DEMS].$$

$\delta LWP_1 \approx 380 \, \delta R_{19v}/R_{19v}$ (mg/cm^2) with a maximum < 38 mg/cm^2 and $\delta LWP_2 \approx 160 \, \delta DEMS/DEMS$ (mg/cm^2) with maximum < 16 mg/cm^2; δLWP_1 has similar wind speed dependence to δLWP_2 because the relative error of R_{19v} is small. From Figure 3 we see that relatively larger values of $\delta DEMS$ occur when near-surface wind speed is small. If the uncertainties of wind speeds are < 5 m/s, the
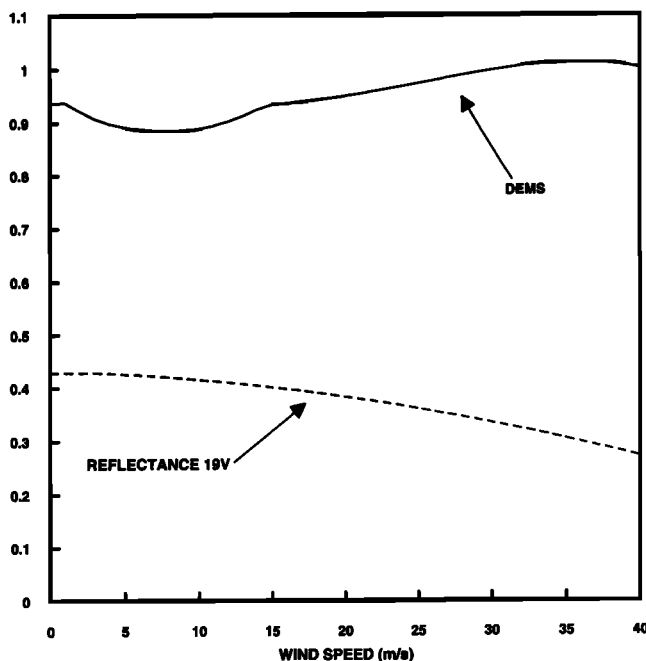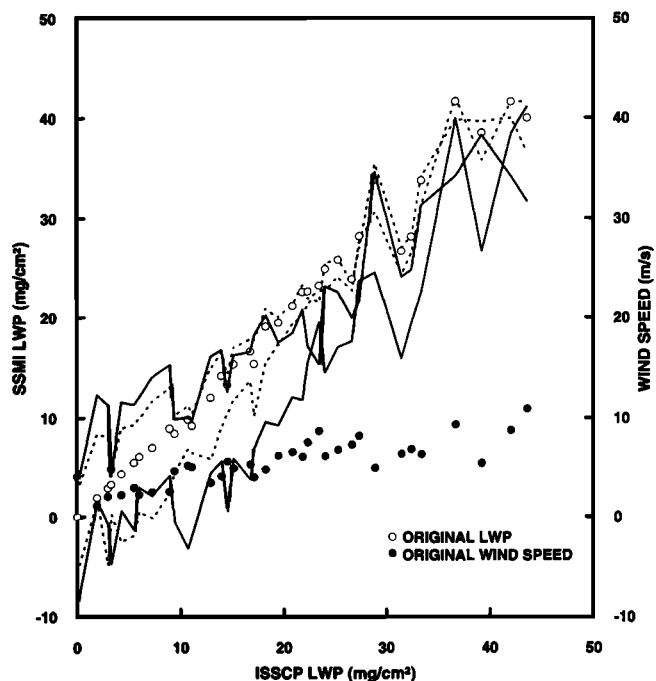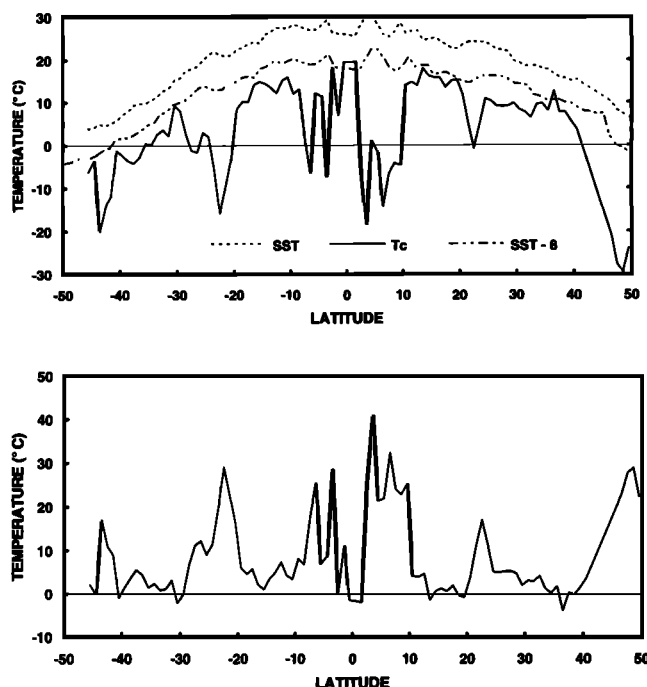

Figure 4. LWP variations with different wind speed errors. Open circles are original LWPs, and solid circles correspond to the original estimated wind speeds. Dotted curves are the LWPs with ± 2 m/s wind speed errors and solid curves are those with ± 5 m/s errors.

relative errors of DEMS will be < 6% and δLWP_2 will be less than 10 mg/cm^2. *Goodberlet et al.* [1990] estimate that the wind speed uncertainties in their method are < 5 m/s for weather conditions indicated by a flag value is equal to 1 and < 2 m/s for flag is equal to 0. As LWP increases, the importance of the surface radiation decreases and the relative uncertainty associated with wind speed uncertainties decreases. Moreover, if the wind speed uncertainties are roughly constant, the absolute uncertainty of LWP will probably decrease with increasing LWP because larger values of LWP are more likely to be associated with larger surface wind speeds (stormy conditions).

Figure 4 shows the sensitivity of the retrieved LWP values, compared with matched ISCCP values, to variations in W of ± 2 and ± 5 m/s. Uncertainties in LWP are generally small for wind speed uncertainties < 2 m/s (Goodberlet et al.'s condition flag is equal to 0) with the largest uncertainties occurring in the DEMS-minimum region (compare Figure 3). For larger uncertainties of 5 m/s (Goodberlet et al.'s condition flag is equal to 1), significant errors (about 5 mg/cm^2) in LWP can arise, particularly at lower values. The comparison of SSM/I and ISCCP values of LWP suggests that the uncertainties associated with wind speeds from 0 to 10 m/s are not large (but not negligible), indirectly confirming Goodberlet et al.'s estimate of their wind speed uncertainties.

When the weather condition flag equals 2 or 3, the winds are usually very strong, which reduces the sensitivity of the LWP retrieval to wind speed uncertainties (compare Figure 3). We find, however, that the values of LWP from SSM/I and ISCCP are poorly correlated in such cases. One explanation is that these cases are also associated with precipitation [*Goodberlet et al.,* 1990], in which case the ISCCP values of cloud-LWP are lower than the SSM/I values. Another factor is that when wind speeds are large (> 10 m/s), wind speeds at cloud level are probably large, too. Although

Figure 3. Sea surface reflectivity R_{19v} and $(\epsilon_{19v} - \epsilon_{19h})/(\epsilon_{37v} - \epsilon_{37h})$ (DEMS) versus wind speed. These two terms vary by less than 10% with different wind speeds. DEMS is a minimum near a wind speed of 8 m/s.

Figure 5. The ISCCP sea surface temperature and various cloud temperatures (in unit degree Celsius) for 217°E 222°E, 50°S 50°N on October 2, 1987. (a) The dotted line is the longitudinal averaged sea surface temperatures (T_s), the solid one is the averaged ISCCP cloud top temperatures, and the dashed line is $T_s - 8$ K. (b) The averaged difference between $T_s - 8$ K and ISCCP cloud top temperature.

SSM/I and ISCCP pixels are colocated to within 30 km, time differences can be as large as 1.5 hours. Under strong wind conditions, such time differences could increase the location mismatch to > 80 km, thereby decreasing the correlation between the two results.

### Effect of Uncertainties in Cloud Liquid Water Temperature

To test the effect of cloud liquid water temperature on the LWP retrieval, we specify its value either as $T_s - 8$ K [after *Greenwald et al.*, 1992] or as the cloud top temperature, T_c, from ISCCP. Because sea surface temperature varies with latitude, even a small quantitative error in cloud liquid water temperature would appear as latitudinal gradient in LWP. We examine the effects in a narrow longitude band (217°E – 222°E, 50°S – 50°N) for October 2, 1987. Results for other cases are basically the same. Figure 5 shows the latitudinal variations of T_s, T_c, and $T_s - 8$ (Figure 5a) and the differences between $T_s - 8$ and T_c (Figure 5b). $T_s - 8$ K is generally a little larger than the cloud top temperature. In storm regions, especially the intertropical convergence zone (ITCZ), the differences between these two temperatures can reach 25°C (even if cloud liquid water temperatures are limited to > 0°C (see below), the differences are still > 15°C). In regions dominated by warm, nonprecipitating clouds, these two temperatures are very similar.

Figure 6 compares the results of the two retrievals as a scatter plot of the individual LWP values. The solid and open circles represent cloud temperature differences (i.e., $T_s - 8 - T_c$) less than and greater than 15°C, respectively. For cloud temperature differences less than 5°C we find that the rms LWP differences are less than 2 mg/cm² in agreement with a theoretical sensitivity estimate (using a method similar to the one in the near-surface wind speed part). Most of the cases where the LWPs differ by more than 10 – 15 mg/cm²

occur when the ISCCP cloud top temperature differs from $T_s - 8$ K by more than about 15°C, particularly in the ITCZ. Because the liquid water absorption coefficients increase with decreasing temperature, it is the coldest liquid water that is more important in the microwave absorption and emission. As the ISCCP cloud top temperatures are significantly lower than $T_s - 8$ K for most pixels, the LWPs retrieved using cloud top temperatures are significantly lower. For cold cloud top temperatures, some portion of the cloud above the freezing level is likely composed of both ice and liquid water, so that proper specification of the effective temperature for such clouds is important to the accuracy of the inferred value of LWP.

We test another alternative: cloud liquid water temperature is taken to be the cloud top temperature when it exceeds 0°C and is set equal to 0°C when cloud top temperature is < 0°C. Figure 7 shows the retrieval scatter plots for this alternative scheme. The differences in LWP decrease (see Figures 6 and 7) from 8 to 6 mg/cm², rms, because the maximum difference in cloud temperatures has been reduced. These results show that while the two definitions of cloud temperature are quantitatively similar for nonprecipitating clouds, the use of ISCCP cloud top temperatures limited to be ≥ 0°C may reduce systematic errors with latitude and season caused by using $T_s - 8$ K. Some error may still persist because some supercooled liquid may occur. For precipitating clouds, which usually have larger vertical extents that makes it hard to define a cloud liquid water temperature, we use the same prescription as for nonprecipitating clouds.

The differences shown in Figure 7 between the two LWP values are still large for some pixels. These cases correspond to thick tropical precipitating clouds, where the value of $T_s - 8$ K is higher than the actual "effective" cloud liquid water temperature and the ISCCP cloud top temperature is lower than actual cloud liquid water temperature. These results suggest a systematic high bias for the
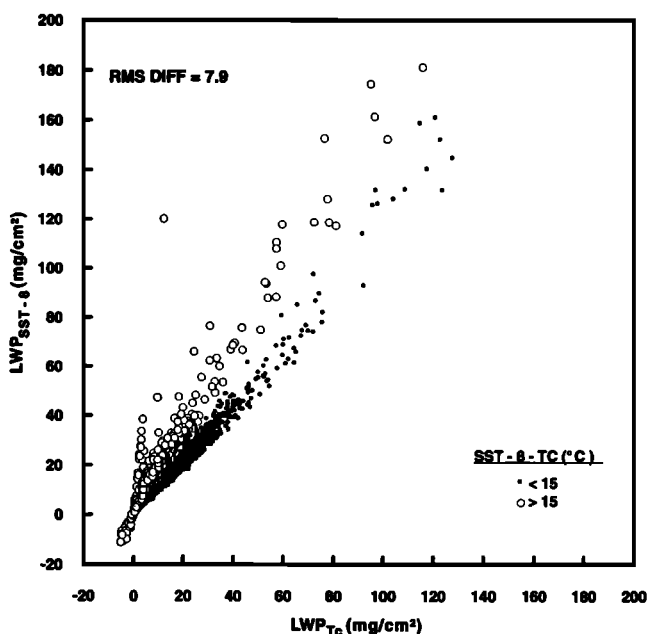
Figure 6. Comparison of LWPs derived from two different specifications of cloud liquid water temperature in a microwave analysis. Abscissa and vertical axis present the LWPs with cloud temperature derived from cloud top temperature and $T_s - 8$ K, respectively. Solid circles reflect cases with temperature differences less than 15°C, while open circles are cases with temperature differences greater than 15°C.
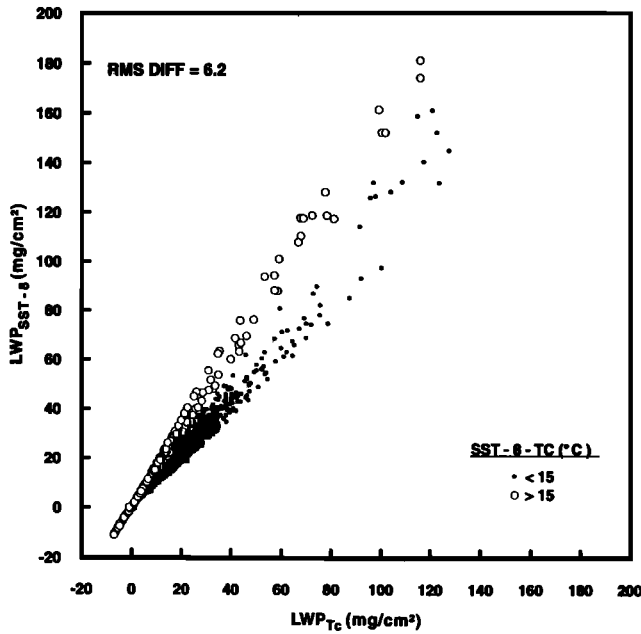
Figure 7. Same as Figure 6 but with cloud liquid water temperatures set to 0°C in all clouds with cloud top temperature less than 0°C.

microwave-based LWP values for tropical clouds and a smaller low bias in LWP values for higher-latitude clouds in the *Greenwald et al.* [1992, 1993] results. Our retrievals can also have systematic bias because cloud top temperature (if Tc ≥ 0°C) is used, but for nonprecipitating clouds the bias is expected to be small. A better method for choosing the cloud liquid water temperature for all types of clouds is needed to reduce this source of systematic error in LWP.

Relation Between LWP and CWV

Equations (6) and (7) show that CWV and LWP are linearly correlated. Any errors in CWV appear as opposite errors in LWP and vice versa. To test the mutual sensitivities of LWP and CWV, we calculate two parameters: δCWV and δLWP for both clear and cloudy scenes, where

$$\delta\text{CWV} = \text{CWV}_{\text{SSM/I cloudy sky}} - \text{CWV}_{\text{SSM/I clear sky}}$$

$$\delta\text{LWP} = \text{LWP}_{\text{SSM/I cloudy sky}} - \text{LWP}_{\text{ISCCP}}.$$

$\text{CWV}_{\text{SSM/I cloudy sky}}$ and $\text{LWP}_{\text{SSM/I cloudy sky}}$ are obtained by solution of equations (6) and (7), together, while $\text{CWV}_{\text{SSM/I clear sky}}$ is obtained from equation (6) with LWP = 0. Under cloudy conditions the latter is not the real CWV of the atmosphere, but this value indicates the error made in retrieval of CWV if clouds are present but unaccounted for in the analysis. Figure 8 shows a scatterplot of δLWP versus δCWV for the October 1987 data in the test region; a similar result is obtained for other weather conditions and cloud types as long as the cloud top temperatures are > 0°C. Under clear conditions (Figure 8a) a linear relationship between δCWV and δLWP is observed as expected. This result represents either the error in CWV that would be produced by a small undetected amount of liquid water cloud contamination or the spurious value of LWP retrieved when there is an error in CWV. The error in CWV caused by cloud contamination is usually small, only about 0.5 g/cm² for atmosphere-LWP = 15 mg/cm² (note that partial cloud cover of the SSM/I field of view can contribute such values of atmosphere-LWP, the LWP

averaged over both cloudy and clear portions). However, the sensitivity of LWP is rather large: a CWV error of 1 g/cm² (relative error approximately 25% in tropics) produces an error in LWP of almost 30 mg/cm².

Under cloudy conditions (Figure 8b) the results are very similar, but there is more scatter because the CWV in cloudy regions may not be the same as in clear regions (as assumed by *Wittmeyer and Vonder Haar* [1994] and *Gaffen and Elliott* [1993]) and the ISCCP and SSM/I disagree somewhat. The scatterplot in Figure 8b shows a shift to the left indicating that CWVs are overestimated under cloudy conditions, if it is assumed to be clear, as expected. Both clear and cloudy tests suggest that the uncertainties in retrieved LWP for warm, nonprecipitating clouds, which generally have values < 30 mg/cm², will be significant if uncertainties of CWV are > 1 g/cm².
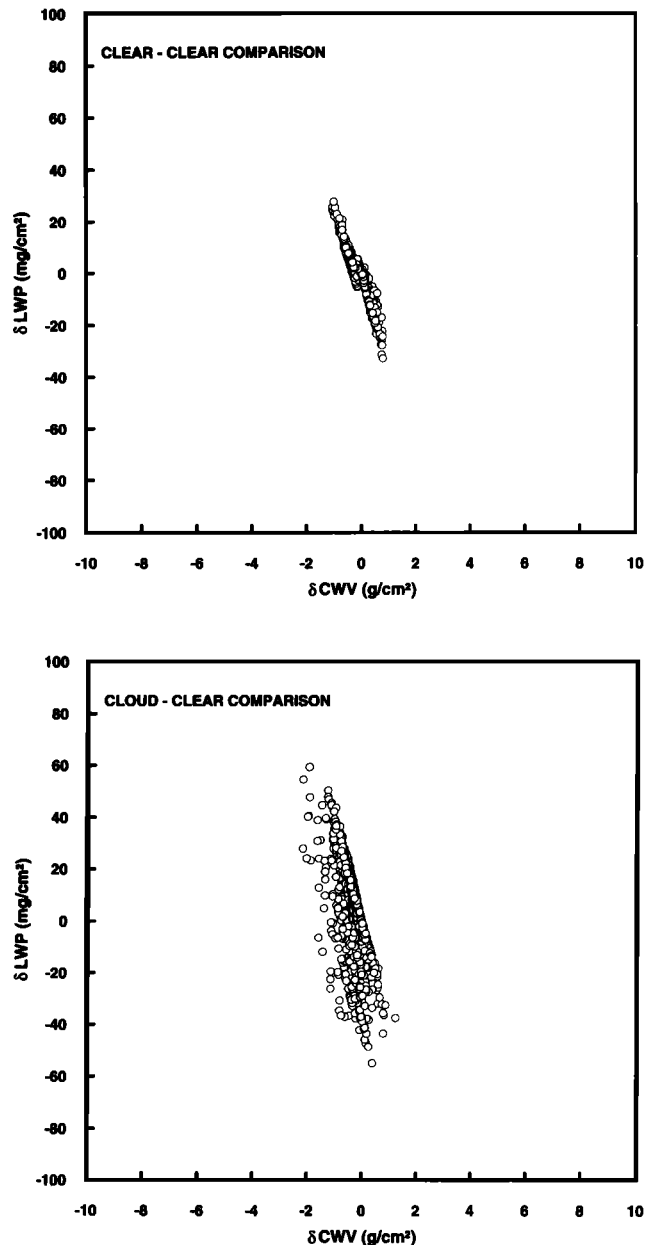

Figure 8. The δCWV versus δLWP (definition in text). (a) Clear sky cases where slope of best fit straight lines is approximately -30 mg/g. (b) Cloudy sky cases with almost the same slope.

Using the same method described in the near-surface wind speed part, we define the sensitivity as

$$S_1 = \delta LWP/\delta CWV = -k^{V19}/k^{L19}$$

$$S_2 = \delta LWP/\delta CWV = -(k^{V37} - k^{V19})/(k^{L37} - k^{L19}).$$

S_1 is approximately -30 mg/g and S_2 is approximately -0.7 mg/g. The different sensitivities of equations (6) and (7) reflect the fact that the 37-GHz measurements are much more sensitive to liquid water than the 19-GHz ones [e.g., *Petty*, 1990]. If relative errors are considered, then assuming $D^L = \delta LWP/LWP$ and $D^V = \delta CWV/CWV$, we have $D^L = S\ CWV\ D^V/LWP$, where S is the sensitivity. Because CWV changes less than LWP, relative LWP errors will decrease as LWP increases.

Comparison of ISCCP and SSM/I LWP Values

Equation (7) for retrieving LWP must be adjusted to account for systematic errors in the sea surface emissivity model (including bias errors from wind speed determinations), uncertainties in the absorption coefficients of water vapor, and uncertainties in SSM/I calibration, as discussed by *Spencer et al.* [1989], *Petty* [1990], and *Liu and Curry* [1993]. Comparison of *Pandey and Kakar's* [1982] expression and *Petty's* [1990] model for surface emissivity shows small systematic differences. Since the precise temperature dependence of the water vapor absorption coefficients used to retrieve CWV is only poorly known [*Liu et al.*, 1992; *Greenwald et al.*, 1993], there may be systematic errors in LWP caused by systematic errors in CWV.

We can remove systematic retrieval errors by adjusting the water vapor term in equation (7) so that LWP = 0 when no clouds are present. By matching SSM/I and ISCCP pixels that are clear, we can calculate CWV from equation (6) and adjust the water vapor absorption coefficients in equation (7) until LWP = 0 on average. This tuning procedure provides a more accurate treatment for clear sky cases and eliminates some biases in LWP estimation [compare *Greenwald et al.*, 1993]. However, systematic differences in CWV between clear and cloudy conditions [*Gaffen and Elliott*, 1993; *Wittmeyer and Vonder Haar*, 1994], especially when CWV values are higher than 35 mg/cm^2, imply a bias in LWP of about 0.3 mg/cm^2 (Note that from Gaffen and Elliott and Wittmeyer and Vonder Haar's papers we estimate that the CWV differences are about 10% when CWV is above 35 mg/cm^2). Because of this procedure the absorption coefficients used hereinafter are actually effective ones that vary with location and time. Similar tuning methods are used by other authors [*Petty*, 1990; *Liu et al.*, 1992; *Liu and Curry*, 1993; *Greenwald et al.*, 1993].

Regional comparisons. A regional comparison of LWP values from ISCCP and SSM/I is made first for October 1987 in the area bounded by 31°N – 36°N and 238°E – 243°E, the same area used by *Greenwald et al.* [1992, 1993]. This comparison is restricted to warm (cloud top temperatures > 0°C), nonprecipitating clouds with calm sea surface.

Since errors in CWV can significantly affect the LWP retrieved from the microwave measurements, it is difficult to judge whether clear conditions prevail from microwave measurements alone. On the other hand, the ISCCP cloud detection uses such small radiance thresholds over oceans [*Rossow and Garder*, 1993a; *Wielicki and Parker*, 1992] that possible cloud contamination is equivalent to atmosphere-LWP < 0.2 mg/cm^2. We assess how well the SSM/I LWP values approximate zero by collecting all SSM/I observations matched with clear ISCCP pixels. Figure 9 shows the SSM/I clear

CLEAR SKY SSMI LWP

CLEAR SKY SSMI LWP
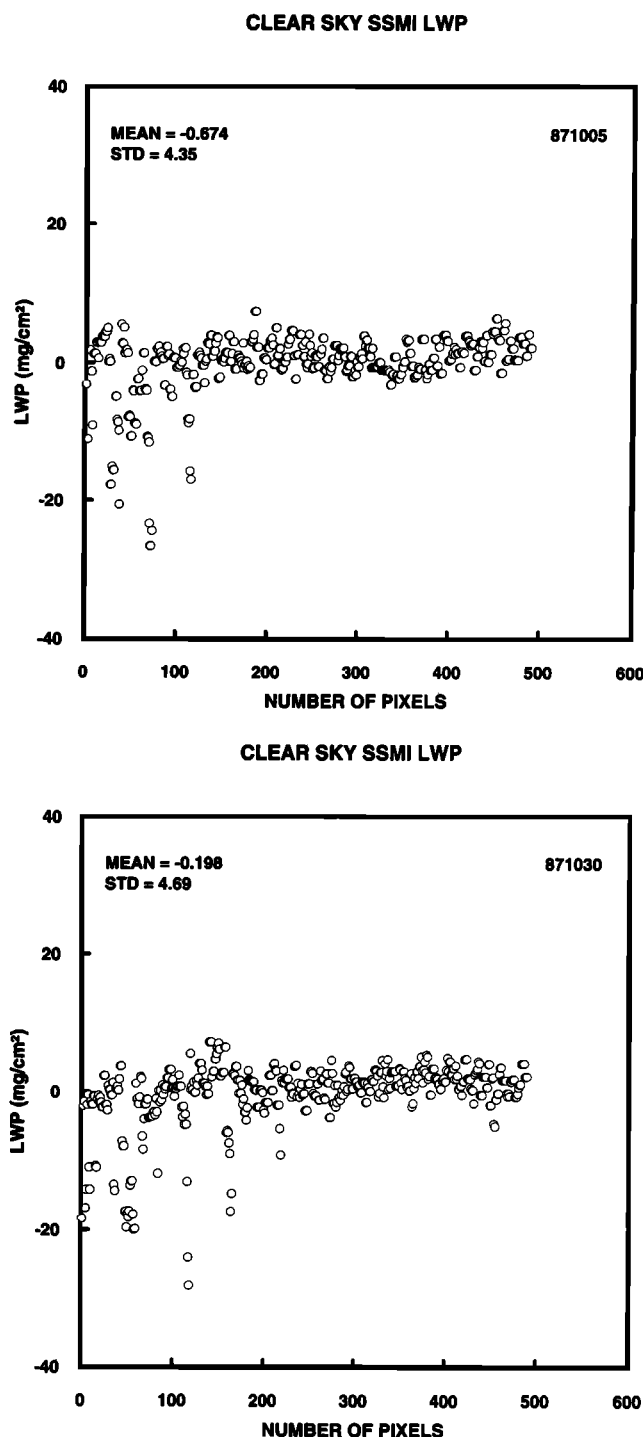
Figure 9. Clear sky LWP derived from the SSM/I data. Abscissas are the pixel numbers, and vertical axes are LWP. Mean and standard deviation also present. (a) Results from October 5, 1987. (b) Results from October 30, 1987.

sky values of LWP for October 5 and 30, 1987, when average cloud cover was about 9 and 14%, respectively (in other words, the regional cloud cover is not zero precisely, but we include in the figure only those results matched with clear ISCCP pixels). The abscissa indicates arbitrary pixel numbers. There are numerous negative values of cloud-LWP in Figure 9, but the average LWPs are both near zero, -0.674 and -0.198 mg/cm^2, respectively. When SSM/I values of LWP for clear pixels are examined for times when the regional

cloud cover is higher than 70%, the average LWP is still small but slightly positive. The increase can be understood because the actual ISCCP pixel size is about a factor of 4 – 5 smaller than the SSM/I pixel size; thus even though the ISCCP indicates no cloud in a particular pixel, the SSM/I measurements may include some clouds. This effect will also be produced by location mismatches.

Combining these results with other cases (not presented here) and our global survey, we find that when cloud cover is negligible according to ISCCP, the average SSM/I value of LWP varies with location but is generally near zero because of our tuning. We interpret the scatter of individual LWP values about zero to be caused by remaining errors in surface properties and CWV. Some additional discussion can be found in the work of *Curry et al.* [1990]. This variation of LWP values about zero defines an intrinsic "noise level" in the SSM/I values of LWP of about 7 mg/cm², rms. This uncertainty in LWP is also equivalent to a finite cloud detection sensitivity for SSM/I measurements.

Under partially cloudy conditions the cloud-LWPs of the two methods do not agree well because of the differences in pixel size between SSM/I and ISCCP. In these conditions we think that the microwave results would best be interpreted to represent atmosphere-LWP. Even though comparisons of satellite and ground-based observations indicate that the occurrence of small-scale, broken clouds constitute only 25 – 35% of the cases, globally [*Rossow et al.*, 1993; *Tian and Curry*, 1989], subtropical marine clouds probably have more broken clouds than other places [cf., *Wielicki and Parker*, 1992, and references therein].

We expect good agreement between the SSM/I and the ISCCP results when regional cloud cover is relatively high and the clouds are warm and nonprecipitating. Such cases are collected on October 1, 8, 12, 13, 14, 15, 22, 23, and 29. Figure 10 shows a scatterplot of cloud-LWPs from ISCCP and SSM/I. The error bars represent the spatial standard deviation of cloud-LWP in the ISCCP and SSM/I images. From this figure it can be seen that the two retrieval methods are in good agreement. The biases in the work of *Greenwald et al.* [1992, 1993], using a different tuning process, are not found here. The differences between the two cloud-LWPs, which are much less in magnitude than the spatial standard deviations, are probably associated with the time and space mismatches between the ISCCP and the SSM/I data sets. These results are also consistent with other results [*Lojou et al.*, 1991; *Greenwald et al.*, 1992, 1993].

Global comparisons. The global results cover all ocean longitudes for latitudes 50°S – 50°N in November 1987. In the global LWP estimation the CWV absorption coefficients in equation (7) are not constant because of their dependence on temperature [*Liebe*, 1985; *Tjemkes et al.*, 1991; *Greenwald et al.*, 1993]. Our retrieval procedure is as follows: (1) Use equation (6) to retrieve CWV under clear sky conditions determined by matched ISCCP pixels. Values of T_s are taken from matched ISCCP pixels and the surface wind speed is retrieved using the method of *Goodberlet et al.* [1990]. (2) Under the same conditions in step 1, use equation (7) to tune the CWV absorption coefficients in each 2.5° × 2.5° grid box to obtain daily and monthly average values of LWP = 0. (3) Use the averaged, tuned CWV absorption coefficients, the adjusted CWV retrieved in step 1 and equation (7) to retrieve LWP for all pixels, clear and cloudy. As before, the T_s and cloud liquid water temperatures (= Tc as long as Tc ≥ 0°C, = 0°C otherwise) come from the ISCCP values and the wind speed is retrieved using Goodberlet et al.'s method.

To understand the retrieved LWP values, we consider four sets of frequency histograms which separate the global results into three climatological regimes, tropical (20°S to 20°N) and northern and southern hemisphere midlatitudes (20° to 50°). We classify each SSM/I pixel as clear or cloudy according to the matched ISCCP
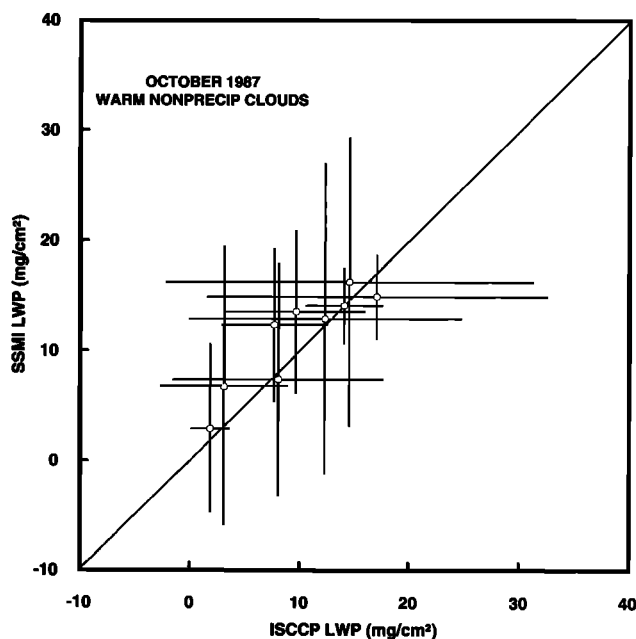

Figure 10. Comparison of ISCCP LWP and SSM/I LWP for warm clouds on October 1, 8, 12, 13, 14, 15, 22, 23, and 29, 1987. Error bars are the spatial variations of LWP in both ISCCP and SSM/I images in terms of one standard deviation above and below the mean values.

pixel; cloudy pixels are further classified by the ISCCP cloud top temperatures as warm (T_c ≥ 0°C) and cold (T_c < 0°C) clouds and by Goodberlet et al.'s microwave indicator of precipitation (Table 1, rain flag = 2 or 3, nonprecipitating, rain flag = 0 or 1). Figure 11 shows the LWP values for clear conditions (the ISCCP LWP is identically zero by definition and is not shown). The mean values are almost zero (because of the tuning); the standard deviations are of the same magnitude as the errors we discussed before (Table 2; hereinafter all means and standard deviations of histograms are given in Table 2).

Figure 12 shows the LWP values for warm, nonprecipitating clouds. Since these values are from SSM/I pixels matched with cloudy ISCCP pixels, the values represent cloud-LWP. The ISCCP histograms show no values below zero (by definition) and a large frequency at the smallest LWP values, indicating a large amount of cloudiness with very low values of cloud-LWP, whereas the SSM/I histograms show a frequency peak near zero LWP with significant numbers of negative values. The SSM/I histograms are shifted toward positive values, however, and the average values from SSM/I and ISCCP show good agreement (Table 2). The two histograms would be very similar if all the negative values in the SSM/I histogram were added into the smallest positive category (although some small positive values would also need to be shifted into the smallest category). This comparison demonstrates that the optical and microwave LWPs are quantitatively similar for the type of clouds expected to show the best agreement.

Note that the shape of the SSM/I LWP histograms in Figures 11 and 12 are nearly the same. This result is symptomatic of the low sensitivity of the microwave to low values of LWP, especially given the uncertainties in sea surface temperature, surface wind speed, cloud liquid water temperature, and CWV. In effect, the microwave signal for clouds with cloud-LWP < 7 mg/cm² (equivalent to visible optical thicknesses < 11) is indistinguishable from clear conditions. The ISCCP distributions indicate that such clouds constitute more than half of the low, warm clouds (Figure 12). Other types of clouds are discussed in section 5.
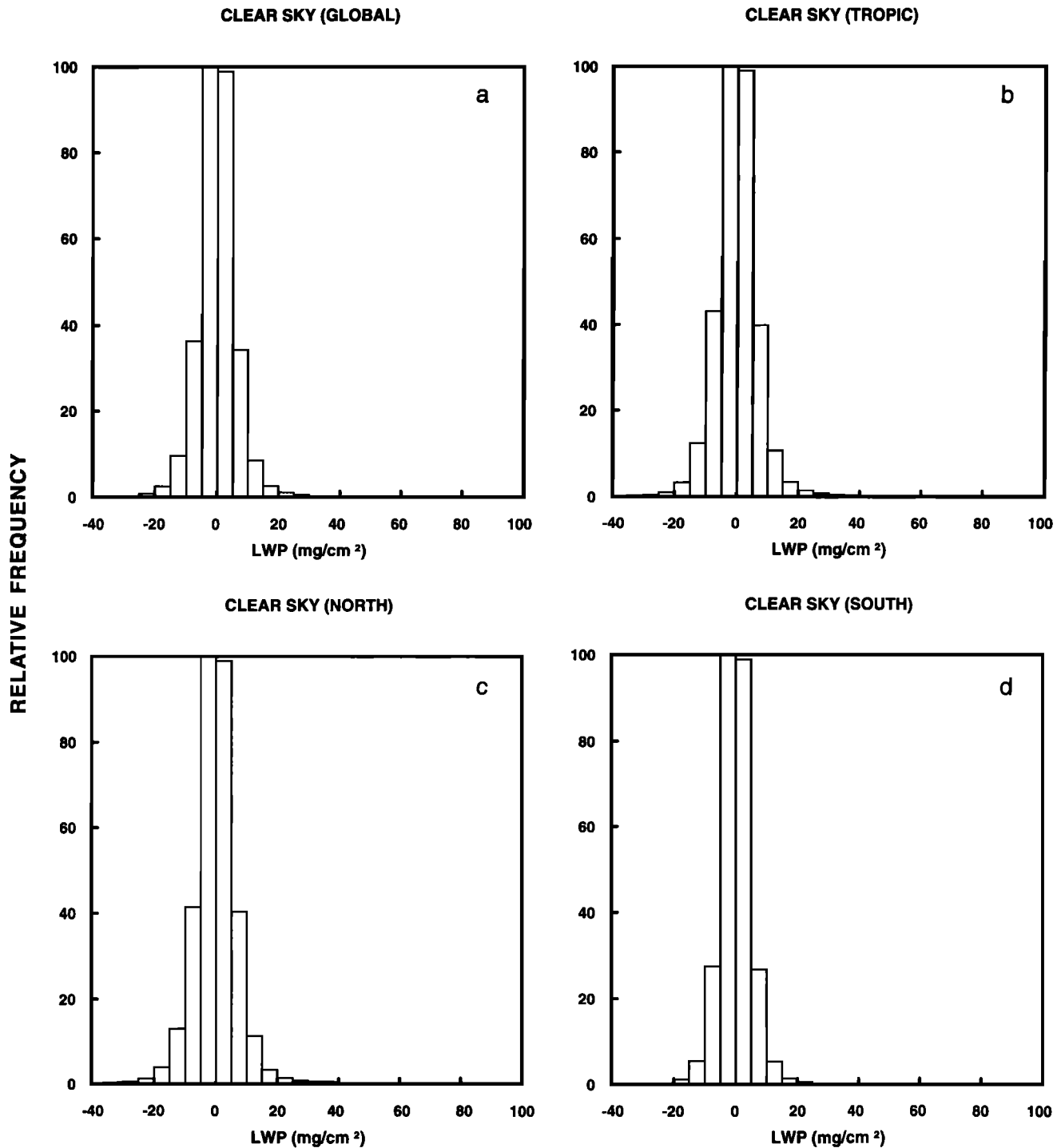
Figure 11. Relative frequency (percent) of clear sky LWP values estimated from SSM/I for (a) global, (b) tropical, (c) northern, and (d) southern hemispheric midlatitude regimes. Means and standard deviations are given in Table 2.

5. Global LWP Distribution

Near-global LWP results are obtained from one month of SSM/I data matched to ISCCP pixels; we obtain a proper measure of cloud-LWP by collecting SSM/I measurements matched with cloudy ISCCP pixels. The results are separated to compare LWP values for warm (W) and cold (C) clouds, nonprecipitating (NP) and precipitating (P) clouds, and combinations of these for tropical and midlatitude regions. ISCCP cloud top temperatures at 0°C separate

warm from cold clouds. Flag values of 2 and 3 in the wind speed model [*Goodberlet et al.*, 1990] are used to indicate the presence of precipitation. Brightness temperature simulations for precipitating clouds find that this threshold corresponds to a rainfall rate about 0.3 to 0.5 mm/h for cold clouds and slightly higher for warm clouds, which is about the same magnitude as the value used by *Bauer and Schiluessel* [1993]. At present, validation of this rainfall detector is impractical because there are no good surface-based rainfall observation systems over oceans [*Arkin and Ardanuy*, 1989]. Other

Table 2. Mean and Standard Deviation of ISCCP AND SSM/I WPs

	Global	Tropical	Northern Hemisphere Midlatitude	Southern Hemisphere Midlatitude
Clear sky	N/A	N/A	N/A	N/A
	0.016 ± 6.457	0.025 ± 7.028	0.018 ± 7.17	0.003 ± 5.379
Warm nonprecipitating clouds	4.755 ± 7.205	4.814 ± 7.588	5.263 ± 9.214	4.630 ± 6.503
	4.943 ± 9.283	4.437 ± 9.024	5.189 ± 9.556	5.308 ± 9.423
Cold nonprecipitating clouds	9.897 ± 14.83	9.662 ± 15.93	15.59 ± 20.74	9.539 ± 13.59
	4.785 ± 9.888	1.915 ± 7.588	4.279 ± 9.919	6.133 ± 10.51
Warm precipitating clouds	8.354 ± 12.36	7.250 ± 11.93	10.22 ± 15.14	9.806 ± 12.07
	48.40 ± 39.48	49.52 ± 38.76	62.40 ± 38.12	42.52 ± 39.96
Cold precipitating clouds	27.17 ± 22.62	24.09 ± 23.63	35.34 ± 24.67	28.57 ± 21.17
	59.79 ± 40.70	51.65 ± 41.91	68.28 ± 38.87	65.02 ± 38.85

Means and standard deviations (in unit mg/cm^2) of LWP histograms (Figures 11, 12, 13, 15 and 16). Each column represents one climatological regime (i.e., globe, tropics, and northern and southern hemispheric midlatitudes), while each row represents different weather conditions, i.e., clear sky, warm or cold, precipitating, or nonprecipitating clouds. Values in the first line of each row are from ISCCP and in the second line from SSM/I. In clear cases, ISCCP values are not available, because ISCCP LWP is exactly zero by definition in these cases.

microwave precipitation detectors [*Liu and Curry*, 1992; *Petty and Katsaros*, 1990] have not been well validated either. Note that although the microwave LWP retrieval scheme we use is designed for nonprecipitating clouds, it can be adapted for precipitating clouds with fair accuracy [*Liu and Curry*, 1993] because scattering by precipitation-sized particles is relatively weak at 19 and 37 GHz [*Wilheit et al.*, 1991; *Liu and Curry*, 1992].

Table 3 gives the relative frequency of all cloud types for the three climate regimes. Globally, just 6.5% of all clouds are precipitating clouds. There are significantly more precipitating clouds in the tropics than in midlatitudes. The importance of the presence of the ice phase (and cloud vertical extent) in precipitation processes is suggested by the much lower probability of precipitation in warm clouds than in cold clouds. Globally, less than 20% of precipitating clouds are warm clouds, while more than 40% of nonprecipitating clouds are warm clouds.

Nonprecipitating clouds, about 60% with cold top temperatures and 40% with warm top temperatures, have low average cloud-LWP values of around 5 mg/cm^2 (Table 2) according to SSM/I [cf., *Liu and Curry*, 1993]. For warm clouds the average cloud-LWP values derived from ISCCP and SSM/I are very similar, while for cold clouds the ISCCP cloud-LWP is significantly different from and almost twice the SSM/I cloud-LWP (Table 2, Figures 12 and 13). Since the optical method is sensitive to both liquid and ice water, the ISCCP cloud-LWP for cold clouds represents a total column water path, equal to the sum of cloud-LWP and the cloud-IWP, where the ice contribution has some uncertainties and is probably an underestimate, as discussed before. The microwave measurements are not sensitive to cloud ice as long as the particle sizes remain small enough [*Wilheit et al.*, 1977; *Adler et al.*, 1991; *Mugnai and Smith*, 1988; *Smith and Mugnai*, 1988]. Based on the agreement between the ISCCP and the SSM/I values for warm clouds, we interpret the SSM/I value in cold clouds as the cloud-LWP and the difference between the ISCCP and the SSM/I values as the cloud-IWP (we emphasize that the uncertainties in IWP retrieval are currently large, because of uncertainty in ice particle size, but these values should represent a proper lower limit on this quantity).

Figure 14 summarizes these results showing the SSM/I and ISCCP monthly, zonal mean values of cloud-LWP for warm (Figure

14a) and cold (Figure 14b) nonprecipitating clouds. All three climatological regimes have similar mean cloud-LWP values for the warm clouds but quite different ones for cold clouds (Figures 12, 13, and 14). Tropical cold clouds have smaller values of cloud-LWP than at higher latitudes, but winter midlatitude clouds have smaller cloud-LWP values than summer midlatitude clouds. The hemispheric contrast in cloud-LWP values, with correspondingly larger values of cloud-IWP in the winter midlatitude clouds, is understandable in terms of seasonal changes of atmospheric temperature and relatively constant cloud top pressure [*Rossow and Schiffer*, 1991]. The reason for the lower cloud-LWP values in the tropics is less certain but may be associated with higher cloud bases in the stratiform components of tropical convective systems. Differences in tropical and midlatitude cloud dynamics may also produce less supercooled liquid water in the tropics than at higher latitudes [*Curry and Liu*, 1992].

Frequency distributions of SSM/I and ISCCP water path values for precipitating clouds are shown in Figures 15 (warm clouds) and 16 (cold clouds). The ISCCP values are about 5 – 7 times less than the microwave values for warm precipitating clouds and about 2 times less for cold precipitating clouds (Table 2). The optical method is sensitive to the small ice particles in the cloud but insensitive to the large precipitation-sized particles, whereas the microwave measurements are insensitive to the ice particles in the cloud and very sensitive to the precipitation-sized particles. The comparison of ISCCP and SSM/I values for these cases indicates an approximate ratio between cloud and precipitation water paths that is useful for evaluating possible errors in the microwave analysis caused by the cloud component. We consider only the microwave values of cloud-LWP for these cases, but note that the microwave retrieval method still produces some large negative values even for these cases. The average cloud-LWP for precipitating clouds is around 30 to 70 mg/cm^2, which is about 10 times larger than for nonprecipitating clouds (Table 2), consistent with other results [*Curry et al.*, 1990; *Liu and Curry*, 1993]. Cold precipitating clouds have somewhat more liquid water than warm precipitating clouds, particularly in summer midlatitudes.

Figures 17 and 18 show the relative frequencies of precipitating clouds in each range of LWP for warm and cold clouds, respectively. Nearly half of the clouds are precipitating when cloud-LWP exceeds
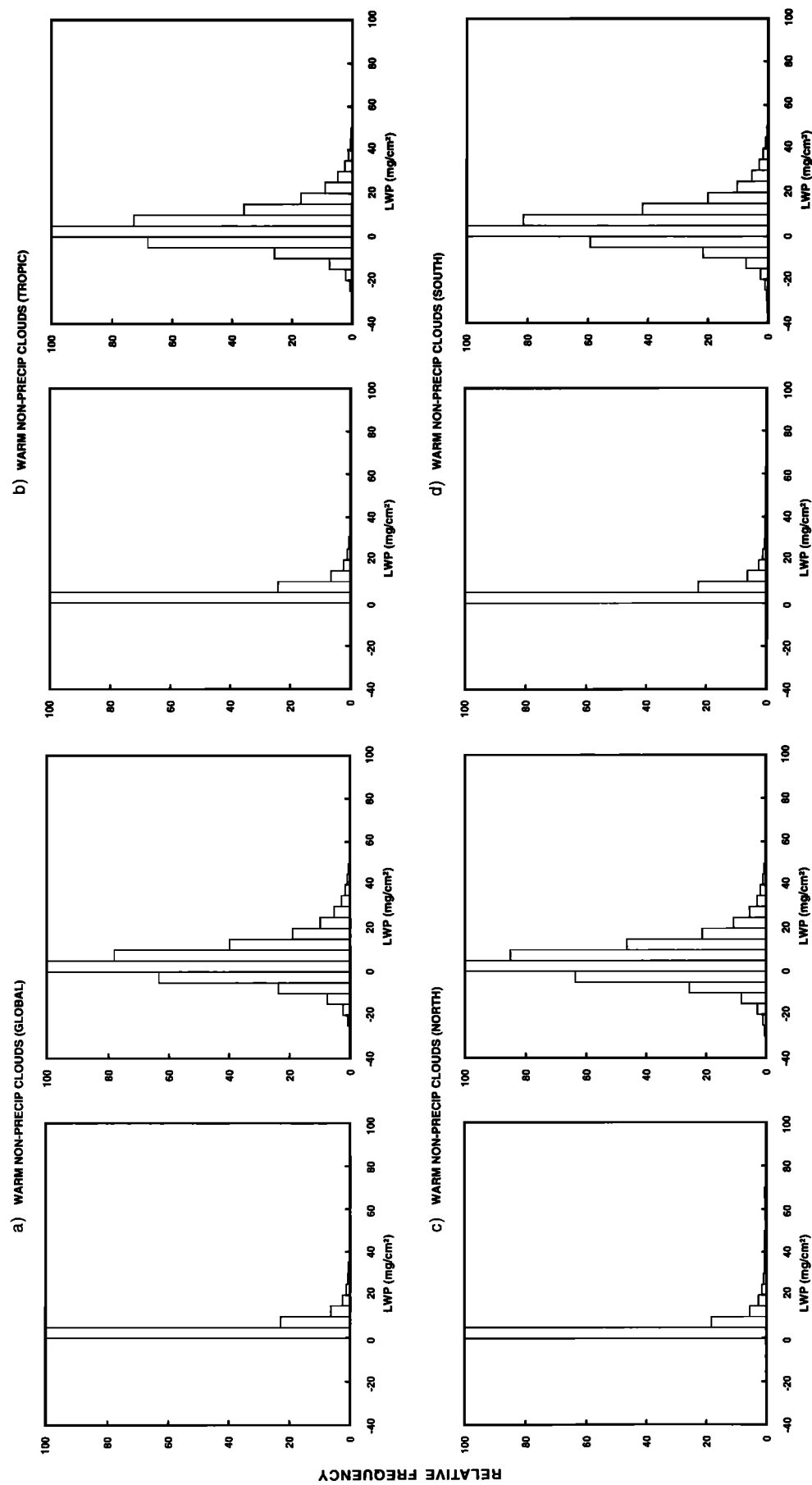
Figure 12. Relative frequency (percent) of LWP for warm, nonprecipitating clouds estimated from ISCCP (left) and SSM/I (right) for (a) global, (b) tropical, (c) northern, and (d) southern hemispheric midlatitude regimes. Means and standard deviations are given in Table 2.

Table 3. Relative Frequencies of Classified Clouds

	Global %	Tropical %	Northern Hemisphere Midlat., %	Southern Hemisphere Midlat., %
P/T	6.5	8.0	6.7	5.4
WP/W	2.4	3.4	2.8	1.6
CP/C	9.1	12.3	10.5	7.6
WP/P	15.0	20.2	20.4	9.8
WNP/NP	41.6	49.5	51.5	36.0

Ratios of amounts of different cloud types. Each column is a climate regime and each row is for different cloud types, where W, C, NP, P, and T are abbreviations of warm, cold, nonprecipitating, precipitating, and total, respectively. Other values (e.g., CNP/NP) can be inferred from the table.

50 mg/cm^2 for warm and 40 mg/cm^2 for cold clouds. The lower threshold for cold clouds, in general, and for tropical clouds, in particular, indicates some differences in the ability of these clouds to produce precipitation. These results are similar to those of *Liu and Curry* [1993]. A precipitation threshold of $40 - 50$ mg/cm^2 is equivalent to a visible optical thickness of about $60 - 80$. Despite the strong relation of average cloud-LWP and the occurrence of precipitation, rainfall rate (RR) is a different physical parameter that may not be so well related to the cloud properties [*Curry et al.*, 1990].

We now return to our primary problem of understanding why the reported microwave values of LWP differ so widely. The answer probably lies in cloud detection (i.e., the definition of cloudy sky and clear sky). The uncertainties in the microwave LWP retrieval (about 7 mg/cm^2), discussed in the previous section, make discrimination between thinner clouds and clear sky very difficult. For example, *Bauer and Schiluessel* [1993] retrieve LWP from SSM/I data only if it is larger than 5 mg/cm^2 (if LWP is less than 5 mg/cm^2, they think it is clear sky and a clear sky CWV retrieval follows), while *Wilheit and Chang* [1980] claimed a smaller LWP uncertainty (about 4 mg/cm^2) for SMMR data. Figure 19 compares the amount of ISCCP clouds with cloud-LWP > 4 mg/cm^2 to the total ISCCP cloud amount. Figure 19 shows that a microwave retrieval including only values of LWP > 4 mg/cm^2 in its average would miss 40% of the clouds, whereas an analysis with no restriction would include about 30% clear sky in the average. Very different values of LWP would be obtained depending on how this issue is treated. Figure 20 shows the monthly, zonal mean values of LWP obtained from SSM/I when all cloud-LWP values are retained (dashed curve), when LWP values for precipitating cases are set to be 50 mg/cm^2, as done by Greenwald et al. [1992, 1993] (solid curve), when all negative LWP values are discarded (dashed-dotted curve), and when clear conditions are included in the average (dotted curve). Comparing cloud-LWP of all clouds (Figure 20, dashed curve) with the LWP for nonprecipitating clouds (Figure 14) shows that the addition of precipitating clouds increases the zonal mean LWP values at higher latitudes and, most especially, in the ITCZ. Notice that setting a constant LWP value for precipitating clouds (Figure 20, solid curve) does not change the overall result much because 50 mg/cm^2 is near the mean LWP for precipitating clouds and the frequency of precipitating clouds is very low (Tables 2 and 3).

However, when all negative values of LWP are discarded (Figure 20, dashed-dotted curve), the average LWP values are 50% larger than the original. Figure 20 dotted curve shows the monthly, zonal mean SSM/I LWP obtained by averaging over clear and cloudy conditions, namely, the atmosphere-LWP. The atmosphere-LWP is

about 2 mg/cm^2 smaller than the cloud-LWP (Figure 20, dashed curve), with a much stronger decrease in the subtropics. These results demonstrate the sensitivity of the microwave results to algorithmic decisions concerning whether clear conditions are to be included in the average LWP. Different algorithmic choices about which low or negative LWP values are included in the statistics will produce very different LWP biases that change with latitude and possibly season. Although the exact threshold in LWP is not clear, the method of Prabhakara et al. uses a cutoff in ratio of brightness temperature deviations of 10.7 and 6.6 GHz to retrieve LWP, which may eliminate most thinner clouds and exaggerate the importance of precipitating clouds in the average LWP. Both Greenwald et al. and Njoku and Swanson have used LWP upper cutoffs which may limit the results more like LWP of nonprecipitating particles. We suspect that these effects may explain some very large differences among the reported results (Figure 1), although the details of these LWP retrievals are not known. Until a better cloud-clear definition for microwave measurements is found, the most reliable interpretation of the SSM/I results is that with all values included in the averages, representing the atmosphere-LWP, the average over clear and cloudy conditions, not the cloud-LWP. The most reliable cloud-LWP values for the optical measurements are for warm, nonprecipitating clouds. Further studies combining the optical and microwave remote sensing methods may be able to provide improved though still crude estimates that separate cloud-IWP, cloud-LWP, and precipitation-LWP.

6. Discussion and Conclusions

We discuss our results, summarize our conclusions, and make several recommendations about the analysis of SSM/I LWP.

1. Uncertainties in sea surface temperatures produce direct errors in microwave LWP values < 1 mg/cm^2, if equation (7) is used instead of a direct absorption-emission form such as equation (6). However, since equation (6) is used to retrieve CWV, errors in T_s can affect LWP retrievals through errors in CWV (see below). Uncertainties in the near-surface wind speed can produce much larger LWP errors (up to 16 mg/cm^2). For nonprecipitating clouds and weather (lower wind speeds), a wind speed uncertainty of about 2 m/s causes errors in LWP of about 5 mg/cm^2, particularly at smaller values of LWP. Note, however, that for climatological mean values of the surface wind speed, errors in wind speed of both signs cause an underestimate of LWP. Both of these results suggest that future microwave instruments should include lower-frequency channels that provide better estimates of the surface properties, such as were available on SMMR, to reduce the errors in CWV and LWP associated with the surface temperature and emissivity (the tropical rainfall measurement mission microwave radiometer and the multifrequency imaging microwave radiometer for the Earth Observation System both have lower-frequency channels).

2. In the emission regime, LWP values retrieved from SSM/I are sensitive to the assumed temperature of cloud liquid water, with the coldest water dominating. In our sensitivity test we find that LWP errors are generally < 2 mg/cm^2 for cloud temperature errors $< 5°C$. For warm, nonprecipitating clouds, use of ISCCP cloud top temperatures produces results that agree well with those estimated using $T_s - 8$ K, as suggested by *Greenwald et al.* [1992]. For other types of clouds, particularly mixed phase clouds, defining an effective cloud temperature needs further study. However, when examining seasonal and latitudinal variations of LWP, the simpler $T_s - 8$ K may introduce spurious dependence. Use of the cloud top temperatures obtained from the operational line scanner (OLS) on the same satellites as SSM/I would provide a better representation
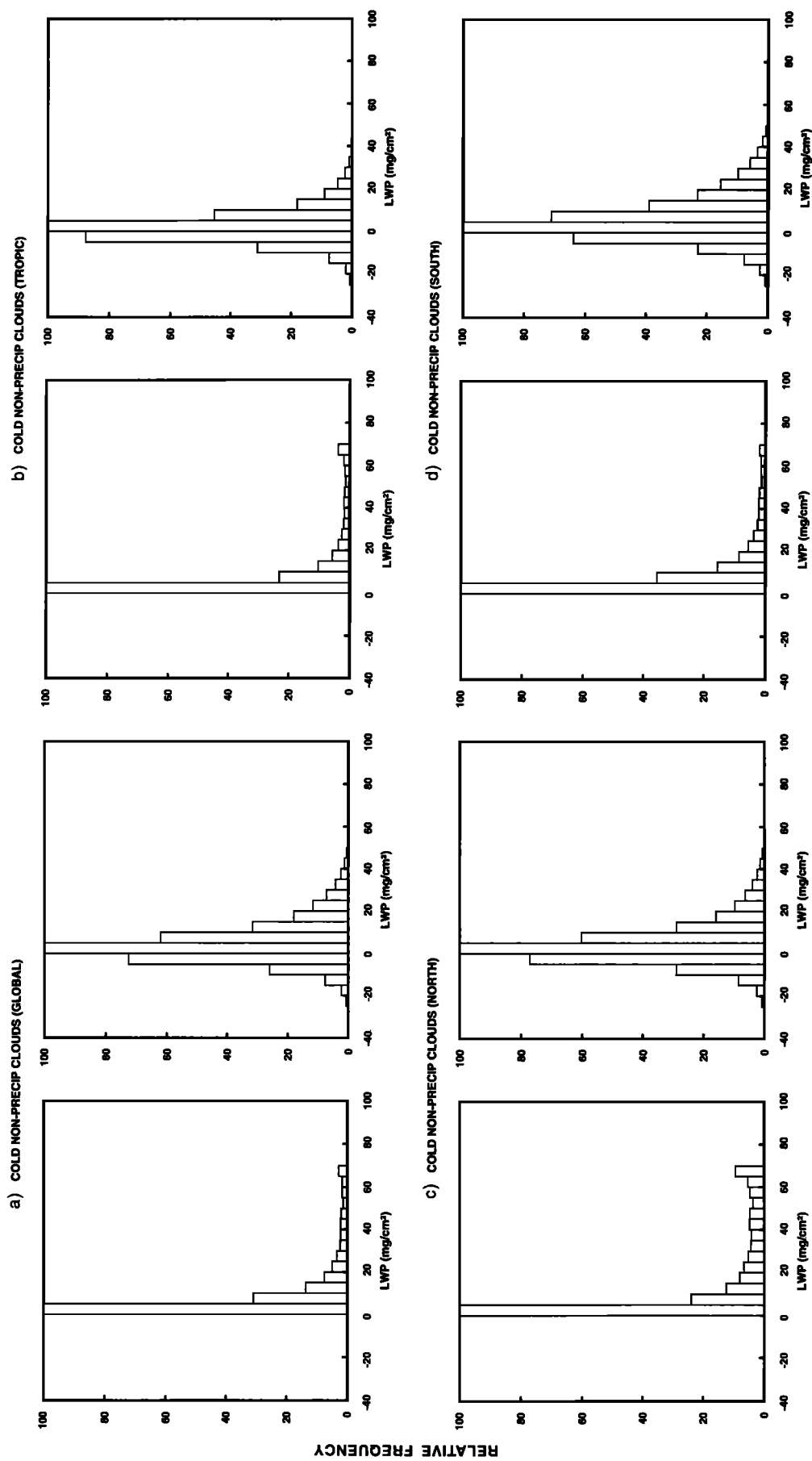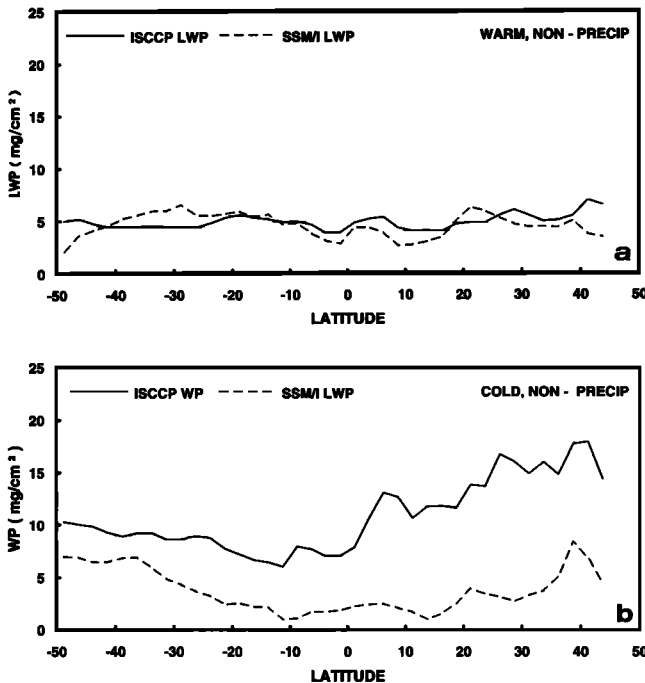
Figure 13. Same as Figure 12 but for cold, nonprecipitating clouds.

Figure 14. Monthly, zonal mean water paths (WPs) derived from both ISCCP (solid line) and SSM/I (broken line) for (a) warm and (b) cold, nonprecipitating clouds.

of the variations of cloud temperature and their effect on the retrieved LWP, especially for nonprecipitating clouds. Note that *Liu and Curry* [1993] use both cloud top temperature and SSM/I brightness temperatures to estimate cloud liquid water temperature, which may confuse variations of water path with water temperature [*Yeh*, 1984].

3. The radiances measured by the SSM/I channels are affected by both CWV and LWP; consequently, retrievals of these quantities are strongly coupled. Errors in the CWV retrieval may obscure the signal from smaller LWP clouds altogether. Our sensitivity test suggests that CWV errors may introduce LWP errors as large as 30 mg/cm^2, which includes almost the whole range of cloud-LWP for nonprecipitating clouds. Most retrieval methods [*Wilheit and Chang*, 1980; *Alishouse et al.*, 1990a, b; *Petty*, 1990; *Katsaros and Brown*, 1991; *McMurdie and Katsaros*, 1991; *Greenwald et al.*, 1992, 1993] couple errors in CWV and LWP. We suggest that a separated CWV and LWP retrieval scheme may be more useful for measurement of cloud-LWP in nonprecipitating clouds [cf., *Takeda and Liu*, 1988; *Curry et al.*, 1990; *Liu and Curry*, 1993]. In the scheme used here, the CWV is retrieved from pixels matched with ISCCP clear pixels and then held fixed for cloudy pixels in the same area and time period. However, this procedure probably introduces a bias in LWP of about 0.3 mg/cm^2.

4. Another problem associated with water vapor effects on the LWP retrievals is that the temperature dependence of the absorption coefficients is poorly known. We found it necessary to tune the retrieval method to remove biases in LWP produced by errors in this quantity by using the clear pixels identified by ISCCP. This tuning also adjusts for any other systematic errors in near-surface wind speeds, surface emissivities, brightness temperatures, and sea surface temperatures. Other authors have also discovered the need for tuning [*Petty*, 1990; *Liu et al.*, 1992; *Liu and Curry*, 1993; *Greenwald et al.*, 1993]. This tuning, together with the sensitivity of CWV retrievals to cloud contamination, implies that CWV from

microwave data sets may contain small systematic errors, in particular following the pattern of cloud cover variations.

5. The average cloud-LWP values obtained from matched ISCCP optical and the SSM/I microwave analyses agree well for overcast, warm, nonprecipitating clouds in calm sea environments. The quantitative consistency is reflected in similar global, zonal, and regional average values of LWP and distribution histograms that are similar in shape except for effects produced by the "intrinsic noise" in the SSM/I results (Table 2, Figures 12 and 14). These results provide cross validation of both the ISCCP retrievals of cloud optical thicknesses and the SSM/I retrievals of cloud-LWP.

6. In this analysis the ISCCP clear and cloudy scene detector is used to understand the SSM/I estimation of cloud-LWP. The low sensitivity of the microwave to very low values of LWP makes it difficult to separate clear and cloudy conditions in microwave observations alone. Simple tests show that different cloud detection schemes are likely to produce significant biases in LWP estimation that vary with latitude and probably season (cf., Figures 19 and 20). We suspect that this is the main reason for large differences in the LWP values previously reported (cf., Figure 1). Since the SSM/I results are insensitive to low LWP clouds, we suggest that the most reliable treatment of microwave results is to include the LWP values retrieved in all microwave pixels in the average and interpret the results as representing the atmosphere-LWP rather than the cloud-LWP. Use of imaging data similar to the ISCCP data, such as from the OLS on the same satellite with the SSM/I, would be useful to improve the cloud-LWP analysis.

7. Our combined SSM/I and ISCCP analysis of global LWP data for November 1987 shows that the cloud-LWP of all nonprecipitating clouds is usually < 30 mg/cm^2 with a mean value of about 5 mg/cm^2. Although these clouds do not contain much liquid water, they are the dominate type in areal coverage and therefore they have the dominant effect on the global radiation budget. Most cold clouds show the microwave signature of precipitation if their cloud-LWP > 40 mg/cm^2, whereas for warm clouds this threshold is at about 50 mg/cm^2 (Figures 17 and 18), suggesting that cold clouds produce precipitation more easily than warm clouds. Only 6 to 7% of all clouds are precipitating, which means they contribute little to the global mean radiative effects of clouds, but they contribute significantly to the total average cloud-LWP, particularly in the ITCZ, because they hold nearly 10 times as much liquid water as nonprecipitating clouds do.

8. By taking the difference between the total-WP retrieved from ISCCP and the cloud-LWP from SSM/I for cold, nonprecipitating clouds, we have obtained the first systematic estimate of cloud-IWP. The results from November 1987 suggest that the ratio of IWP to LWP in cold nonprecipitating clouds shifts significantly with season in midlatitudes (as expected) with IWP being about 3 − 5 mg/cm^2 in the summer hemisphere and about 10 − 15 mg/cm^2 in the winter hemisphere and LWP being about 3 − 8 mg/cm^2 in both hemispheres (Figure 14b). Cold nonprecipitating clouds at midlatitudes contain more cloud-LWP than in the tropics, which may indicate a systematic difference in cloud base levels. These values for IWP are probably lower limits; actually values may be 2 − 3 times larger. At present, because it is very hard to estimate IWP for precipitation-sized ice particles, the zonal mean values of IWP and WP for precipitating clouds are not available. Zonal mean cloud-LWP estimated here shows that tropics and higher latitudes have higher cloud-LWP values, while the subtropics are a minimum.

To study seasonal and interannual variations in cloud-LWP and cloud-IWP, we must combine SSM/I and ISCCP for many more months. Precipitation frequency can also be examined, but estimation of rain rates requires a more sophisticated treatment of the scattering processes.
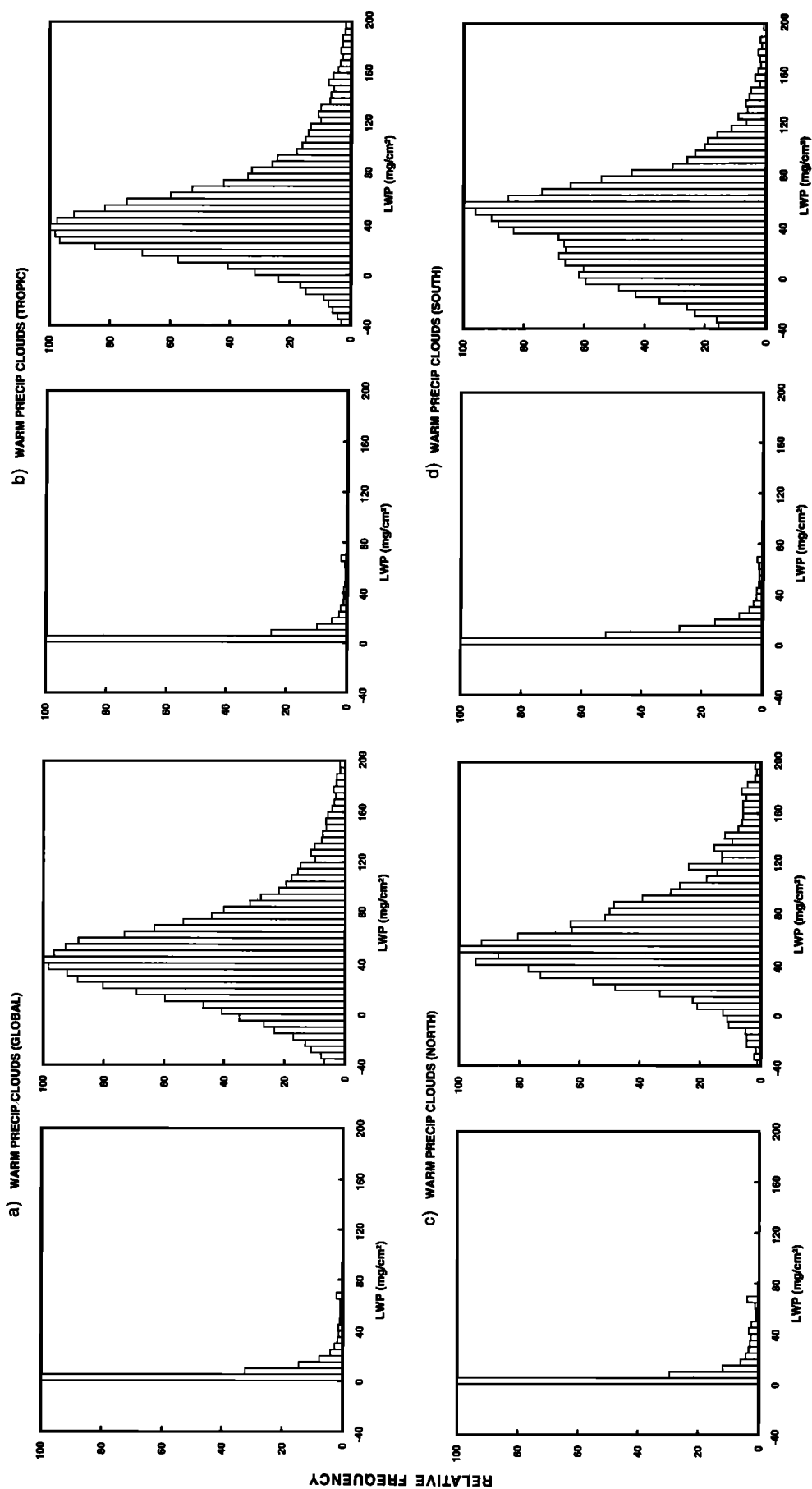
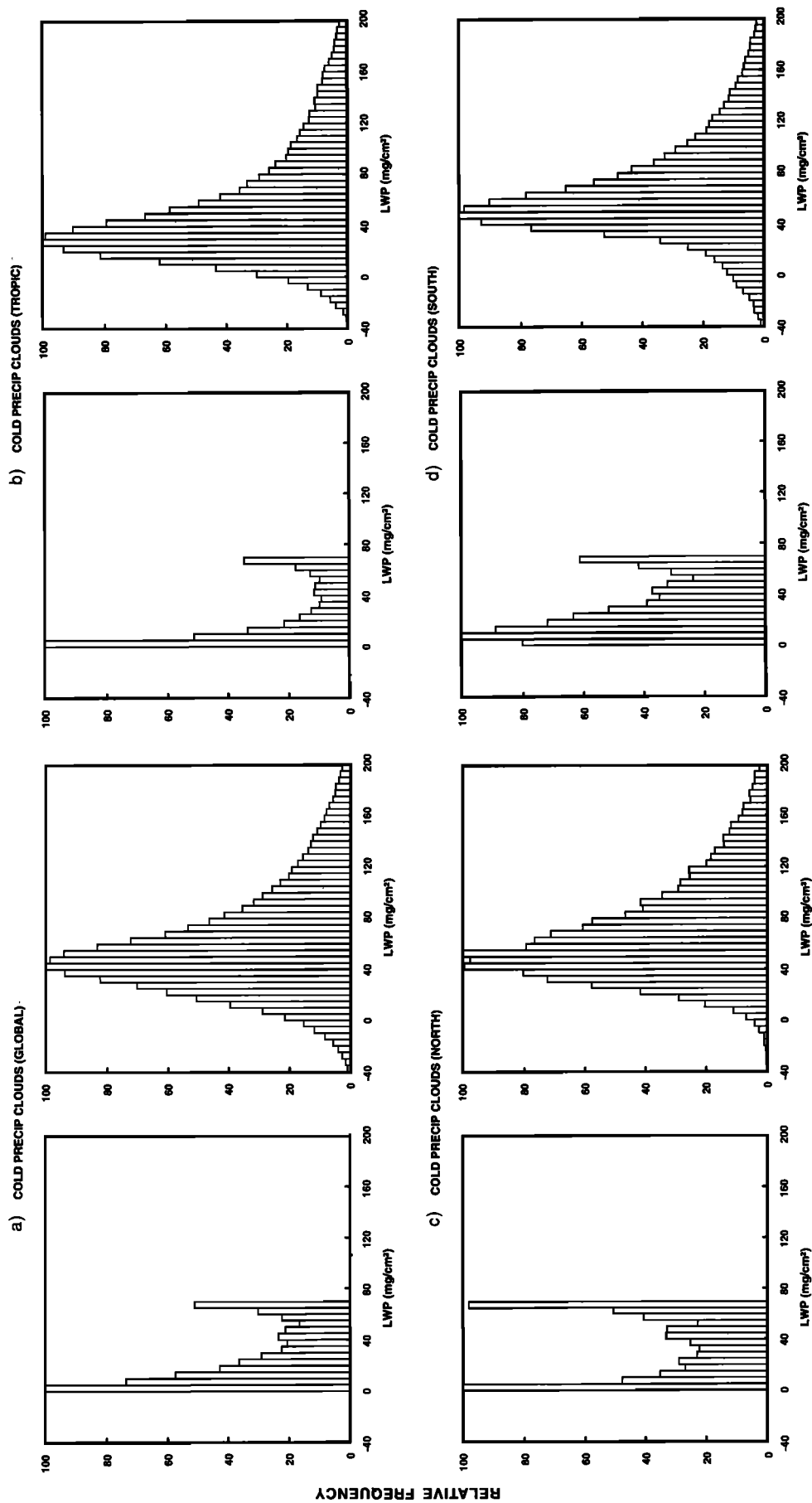Figure 15. Same as Figure 12 but for warm, precipitating clouds.

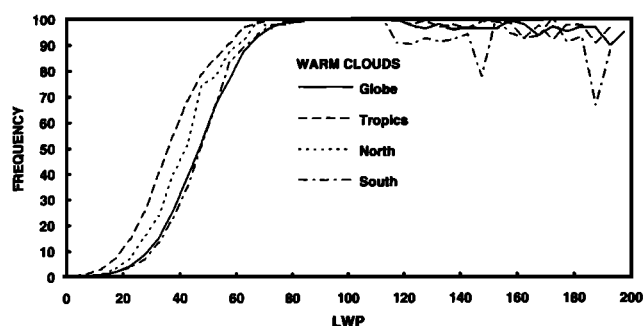Figure 16.　Same as Figure 12 but for cold, precipitating clouds.

Figure 17. Relative frequency (percent) of warm, precipitating clouds to all warm clouds for global (solid line), tropical (dashed line), northern (dotted line), and southern (dashed-dotted line) hemispheric midlatitude regimes.
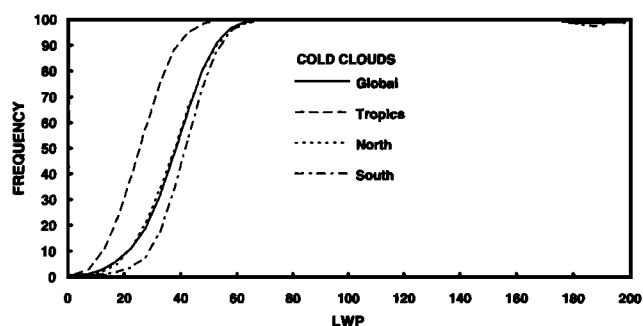

Figure 18. Same as Figure 17 but for cold, precipitating clouds to all cold clouds.
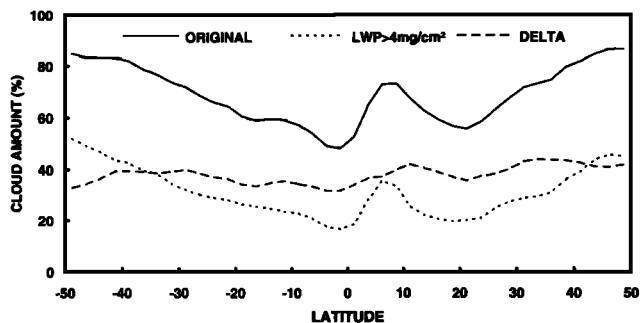

Figure 19. Monthly, zonal mean ISCCP cloud amount (percent) in November 1987. The solid curve represents total cloud amount, the dotted curve is the cloud amount for clouds with LWP > 4 mg/cm², and the dashed curve is the difference between the first two curves.
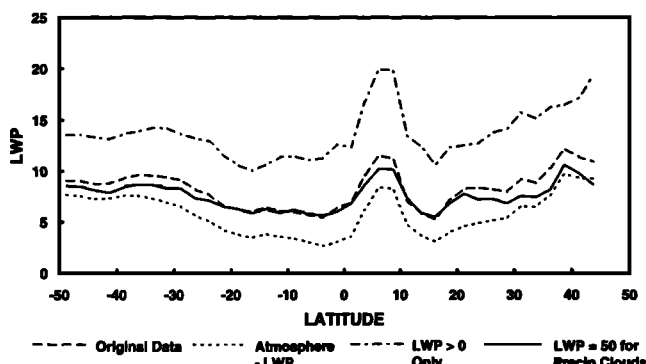

Figure 20. Monthly, zonal mean LWPs derived from SSM/I for only cloudy data (dashed line), the results with LWP = 50 mg/cm² assumed for all precipitating clouds (solid line), the results including only positive LWP values (dashed-dotted line), and the results with both clear and cloudy conditions (atmosphere-LWP, dotted line).

References

Adler, R. F., H.-Y. Yeh, N. Prasad, W.-K. Tao, and J. Simpson, Microwave simulations of tropical rainfall system with a three-dimensional cloud model, *J. Appl. Meteorol., 30*, 924-953, 1991.

Alishouse, J. C., J. B. Snider, E. R. Westwater, C. T. Swift, C. S. Ruf, S. A. Snyder, J. Vongsathorn, and R. R. Ferraro, Determination of cloud liquid water content using the SSM/I, *IEEE Trans. Geosci. Remote Sens., 28*, 817-822, 1990a.

Alishouse, J. C., S. A. Snyder, J. Vongsathorn, and R. R. Ferraro, Determination of oceanic total precipitable water from the SSM/I, *IEEE Trans. Geosci. Remote Sens., 28*, 811-816, 1990b.

Arkin, P. A., and P. E. Ardanuy, Estimating climate-scale precipitation from space: A review, *J. Clim., 2*, 1229-1238, 1989.

Arking, A., The radiative effects of clouds and their impact on climate, *Bull. Am. Meteorol. Soc., 71*, 795-813, 1991.

Bauer, P., and P. Schiluessel, Rainfall, total water, ice water, and water vapor over sea from polarized microwave simulations and the Special Sensor Microwave/Imager data,*J. Geophys. Res., 98*, 20,737-20,759, 1993.

Baum, B. A., B. A. Wielicki, P. Minnis, and L. Parker, Cloud-property retrieval using merged HIRS and AVHRR data, *J. Appl. Meteorol., 31*, 351-369, 1992.

Curry, J. A., C. D. Ardeel, and L. Tian, Liquid water content and precipitation characteristics of stratiform clouds as inferred from satellite microwave measurements, *J. Geophys. Res., 95*, 16,659-16,671, 1990.

Curry, J. A., and G. Liu, Assessment of aircraft icing potential using satellite data, *J. Appl. Meteorol., 31*, 605-621, 1992.

Gaffen, D. J., and W. P. Elliott, Column water vapor content in clear and cloudy skies, *J. Clim., 6*, 2278-2287, 1993.

Gloersen, P., et al., A summary of results from the first Nimbus 7 SMMR observations, *J. Geophys. Res., 89*, 5335-5344, 1984.

Goodberlet, M. A., C. T. Swift, and J. C. Wilkerson, Ocean surface wind speed measurements of the Spacial Sensor Microwave/Imager (SSM/I), *IEEE Trans. Geosci. Remote Sens., 28*, 823-828, 1990.

Greenwald, T. J., G. L. Stephens, and T. H. Vonder Haar, A physically-based retrieval of cloud liquid water from SSM/I measurements, paper prsented at 6th Conference on Satellite Meteorology and Oceanography, Amer. Meteorol. Soc., January. 5-10, Atlanta, Ga, 1992.

Greenwald, T. J., G. L. Stephens, T. H. Vonder Haar, and D. L. Jackson, A physical retrieval of cloud liquid water over global oceans using Special Sensor Microwave/Image (SSM/I) observations,*J. Geophys. Res., 98*, 18,471-18,488, 1993.

Han, Q., Global survey of effective particle size in liquid water clouds, Ph.D. dissertation, 200 pp., Dep. of Geol. Sci., Columbia Univ., New York, 1992.

Han, Q.-Y., W. B. Rossow, and A. A. Lacis, Near-global survey of effective cloud droplet radii in liquid water clouds using ISCCP data, *J. Clim., 7*, 465-497, 1994.

Hansen, J. E., and L. D. Travis, Light scattering in planetary atmospheres, *Space Sci. Rev., 16*, 527-610, 1974.

Heymsfield, A. J., Precipitation development in stratiform ice clouds: A microphysical and dynamical study, *J. Atmos. Sci., 34*, 367-381, 1977.

Heymsfield, A. J., and L. J. Donner, A scheme for parameterizing ice-cloud water content in general circulation models, *J. Atmos. Sci., 47*, 1865-1877, 1990.

Hobbs, P. V., and A. L. Rangno, Ice particle concentrations in clouds, *J. Atmos. Sci., 42*, 2523-2549, 1985.

Hollinger, J. P., J. L. Pierce, and A. Poe, SSM/I instrument evaluation, *IEEE Trans. Geosci. Remote Sens., 28*, 781-790, 1990.

Katsaros, K. B., and R. A. Brown, Legacy of the Seasat mission for studies of the atmosphere and air-sea-ice interaction, *Bull. Am. Meteorol. Soc., 72*, 967-981, 1991.

Klein, L. A., and C. T. Swift, An improved model for the dielectric constant of sea water at microwave frequencies, *IEEE J. Oceanic Eng., OE-2,* 104-111, 1977.

Liebe, H. J., An updated model for millimeter wave propagation in moist air, *Radio Sci., 20,* 1069-1089, 1985.

Liou, N., *An Introduction to Atmospheric Radiation,* Academic, San Diego, Calif., 1980.

Liu, G., and J. A. Curry, Retrieval of precipitation from satellite microwave measurements using both emission and scattering, *J. Geophys. Res., 97,* 9959-9974, 1992.

Liu, G., and J. A. Curry, Determination of characteristic features of cloud liquid water from satellite microwave measurements, *J. Geophys. Res., 98,* 5069-5092, 1993.

Liu, W. T., W. Tang, and F. J. Wentz, Precipitable water and surface humidity over global oceans from special sensor microwave imager and European Center for Medium-Range Weather Forecasts, *J. Geophys. Res., 97,* 2251-2264, 1992.

Lojou, J. Y., R. Frouin, and R. Bernard, Comparison of Nimbus-7 SMMR and GOES-1 VISSR atmospheric liquid water content, *J. Appl. Meteorol., 30,* 187-198, 1991.

Luo, G., X. Lin, and J. A. Coakley Jr., The 11-μm emissivities and droplet radii for marine stratocumulus, *J. Geophys. Res., 99,* 3685-3698, 1994.

McMurdie, L. A., and K. B. Katsaros, Satellite-derived integrated water vapor distribution in oceanic midlatitude storms: Variation with region and season, *Mon. Weather Rev., 119,* 589-605, 1991.

Minnis, P., P. W. Heck, and D. F. Young, Inference of cirrus cloud properties using satellite-observed visible and infrared radiances, II, Verification of theoretical cirrus radiative properties, *J. Atmos. Sci., 50,* 1305-1322, 1993.

Mugnai, A., and E. A. Smith, Radiative transfer to space through a precipitating cloud at multiple microwave frequencies, Part I, Model description, *J. Appl. Meteorol., 27,* 1055-1073, 1988.

Njoku, E. G., and L. Swanson, Global measurements of sea surface temperature, wind speed and atmospheric water content from satellite microwave radiometry, *Mon. Weather Rev., 111,* 1977-1987, 1983.

Pandey, P. C., and R. K. Kakar, An empirical microwave emissivity model for a foam-covered sea, *IEEE J. Oceanic Eng., OE-7,* 135-140, 1982.

Petty, G. W., On the response of the Special Sensor Microwave/Imager to the marine environment—Implications for atmospheric parameter retrievals, Ph.D. dissertation, Dep. of Atmos. Sci., Univ. of Washington, Seattle, 1990.

Petty, G. W., and K. B. Katsaros, Precipitation observed over the South China Sea by the Nimbus -7 Scanning Multichannel Microwave Radiometer during winter MONEX, *J. Appl. Meteorol., 29,* 273-287, 1990 .

Prabhakara, C., C. H. D. Chang, and A. T. C. Chang, Remote sensing of precipitable water over the oceans from Nimbus 7 microwave measurements, *J. Appl. Meteorol., 21,* 59-68, 1982.

Prabhakara, C., I. Wang, A. T. C. Chang, and P. Gloersen, A statistical examination of Nimbus 7 SMMR data and remote sensing of sea surface temperature, liquid water content in the atmosphere and surface wind speed, *J. Clim. Appl. Meteorol., 22,* 2023-2037, 1983.

Rossow, W. B., and L. C. Garder, Cloud detection using satellite measurements of infrared and visible radiances for ISCCP, *J. Clim., 6,* 2341-2369, 1993a.

Rossow, W. B., and L. C. Garder, Validation of ISCCP cloud detections, *J. Clim.,* 2370-2393, 1993b.

Rossow, W. B., and A. A. Lacis, Global, seasonal cloud variations from satellite radiance measurements. II, Cloud properties and radiative effects, *J. Clim., 3,* 1204-1253, 1990.

Rossow, W. B., and R. A. Schiffer, ISCCP cloud data products, *Bull. Am. Meteorol. Soc., 72,* 2-20, 1991.

Rossow, W. B., L. C. Garder, and A. A. Lacis, Global, seasonal cloud variations from satellite radiance measurements. Part I: Sensitivity of analysis, *J. Clim., 2,* 419-458, 1989.

Rossow, W. B., L. C. Garder, P. J. Lu, and A. W. Walker, International Satellite Cloud Climatology Project (ISCCP) Documentation of Cloud Data, *WMO/TD-266 (Revised),* World Meteorol. Organ., Geneva, 1991.

Rossow, W. B., A. W. Walker, and L. C. Garder, Comparison of ISCCP and other cloud amounts, *J. Clim., 6,* 2394-2418, 1993.

Schiffer, R. A., and W. B. Rossow, The International Satellite Cloud Climatology Project (ISCCP): The first project of the World Climate Research Program, *Bull. Am. Meteorol. Soc., 64,* 779-784, 1983.

Slingo, A., S. Nicholls,, and J. Schmetz, Aircraft observations of marine stratocumulus during JASIN, *J. R. Meteorol. Soc., 108,* 833-856, 1982.

Smith, E. A., and A. Mugnai, Radiative transfer to space through a precipitating cloud at multiple microwave frequencies. II, Results and analysis, *J. Appl. Meteorol., 27,* 1074-1091, 1988.

Smith, E. A., A. Mugnai, H. J. Cooper, G. J. Tripoli, and X. Xiang, Foundations for statistical- physical precipitation retrieval from passive microwave satellite measurements I, Brightness-temperature properties of a time dependent cloud-radiation model, *J. Appl. Meteorol., 31,* 506-531, 1992.

Spencer, R. W., A satellite passive 37 GHz scattering-based method for measuring oceanic rain rates, *J. Clim. Appl. Meteorol., 25,* 754-766, 1986.

Spencer, R. W., H. M. Goodman, and R. E. Hood, Precipitation retrieval over land and ocean with the SSM/I: Identification and characteristics of the scattering signal, *J. Atmos. Oceanic Technol., 6,* 254-273, 1989.

Staelin, D. H., K. F. Kunzi, R. L. Pettyjohn, R. Poon, R. Wilcox, and J. W. Waters, Remote sensing of atmospheric water vapor and liquid water with the Nimbus 5 microwave spectrometer, *J. Appl. Meteorol., 15,* 1204-1217, 1976.

Stephens, G. L., The parameterization of radiation for numerical weather prediction and climate models, *Mon. Weather Rev., 112,* 826-867, 1984.

Stephens, G. L., G. W. Paltridge, and C. M. R. Platt, Radiation profiles in extended water clouds. II, Parameterizations, *J. Atmos. Sci., 35,* 2123-2132, 1978.

Takeda, T., and G. Liu, Estimation of atmospheric liquid water amount by Nimbus 7 SMMR data: A new method and its application to the western North-Pacific region, *J. Meteorol. Soc. Jpn., 65,* 931-946, 1987.

Tian, L., and J. Curry, Cloud overlap statistics, *J. Geophys. Res., 94,* 9925-9935, 1989.

Tjemkes, S. A., G. L. Stephens, and D. L. Jackson, Spaceborne observation of column water vapor: SSMI observations and algorithm, *J. Geophys. Res., 96,* 10941-10954, 1991.

Wentz, F. J., SSM/I antenna temperature tapes, *Tech. Rep. 032588,* Remote Sensing Systems, Santa Rosa, CA,1988.

Wentz, F. J., L. A. Mattox, and A. S. Peteherych, New algorithms for microwave measurements of ocean winds: Applications to Seasat and the Special Sensor Microwave Imager, *J. Geophys. Res., 91,* 2289-2307, 1986.

Wielicki, B. A., and L. Parker, On the determination of cloud cover from satellite sensors: The effect of sensor spatial resolution, *J. Geophys. Res., 97,* 12,799-12,823, 1992.

Wielicki, B. A., J. T. Suttles, A. J. Heymsfield, R. M. Welch, J. D. Spinhirne, M.-L. C. Wu, D. O. Starr, L. Parker, and R. F. Arduini, The 27-28 October 1986 FIRE IFO cirrus case study: Comparison of radiative transfer theory with observations by satellite and aircraft, *Mon. Weather Rev., 118,* 2356-2376, 1990.

Wilheit, T. T., and A. T. C. Chang, An algorithm for retrieval of ocean surface and atmospheric parameters from the observations of the scanning multichannel microwave radiometer, *Radio Sci., 15,* 525-544, 1980.

Wilheit, T. T., A. T. C. Chang, M. S. V. Rao, E. B. Rodgers, and J. S. Theon, A satellite technique for quantitatively mapping rainfall rates over the oceans, *J. Appl. Meteorol., 16,* 551-560, 1977.

Wilheit, T. T., A. T. C. Chang, and L. S. Chiu, Retrieval of monthly rainfall indices from microwave radiometric measurements using probability distribution functions, *J. Atmos. Oceanic Technol., 8,* 118-136, 1991.

Wiscombe, W. J., and R. M. Welch, Reply, *J. Atmos. Sci., 43,* 401-407, 1986.

Wiscombe, W. J., R. M. Welch, and W. D. Hall, The effects of very large drops on cloud absorption. I, Parcel models, *J. Atmos. Sci., 41,* 1336-1355, 1984.

Wittmeyer, I. L., and T. H. Vonder Haar, Analysis of the global ISCCP TOVS water vapor climatology, *J. Clim., 7,* 325-333, 1994.

Yeh, H.-Y. M., Comments on "Inference of cloud temperature and thickness by microwave radiometry from space", *J. Clim. Appl. Meteorol., 23,* 1579, 1984.

B. Lin, Department of Geological Sciences, Columbia University, 2880 Broadway, New York, NY 10025.

W. B. Rossow, NASA Goddard Institute for Space Studies, 2880 Broadway, New York, NY 10025.